USE OF A NEUROTROPHIC FACTOR MIMETIC TO BLOCK AMYLOID TOXICITY IN ALZHEIMER'S DISEASE MODELS

A THESIS

Submitted to the Faculty

of the

WORCESTER POLYTECHNIC INSTITUTE

In partial fulfillment of the requirements for the

Degree of Master of Science

in

Biology and Biotechnology

By

Devika Rawal

APPROVED:

David S. Adams, Ph.D.	Elizabeth Ryder, Ph.D.	Daniel G. Gibson, Ph.D.
Major Advisor	Committee Member	Committee Member
WPI	WPI	WPI

ABSTRACT

Alzheimer's disease (AD) is the most prevalent neurodegenerative disease in the world. The most accepted hypothesis for the cause of this disease is the amyloid cascade hypothesis, which postulates that the formation of extracellular neurotoxic amyloid-β (Aβ) binds specific receptors on the surface of neuronal and glial cells to increase cell stress leading to cell death. Our laboratory previously showed that treatment of cultured human SHSY neuronal cells with Aβ increases the cellular levels of two key components (caspases-2 and -3) of the *extrinsic* apoptotic pathway, leading to cell death. The Aβ-induced caspase elevation was blocked by simultaneously treating the cells with a short mimetic of human ependymin neurotrophic factor, hEPN-1, and the hEPN-1 treatment also blocked cell death. This thesis extends the AD investigation to show that treatment of SHSY cells with Aβ may also activate an *intrinsic* apoptotic mitochondrial stress pathway (assaying caspase-9 as a marker enzyme), and that hEPN-1 treatment significantly lowers this activation. In addition, our laboratory previously showed that treating SHSY cells with Aβ increases TUNEL staining, an assay for DNA fragmentation (a hallmark of end stage of apoptosis, and a different apoptotic marker than caspase activation). Treatment with hEPN-1 simultaneously with the Aβ, or 6 hrs post Aβ, significantly lowered the Aβ-induced TUNEL signal. This thesis extended the earlier TUNEL experiments to show that hEPN-1 treatment can significantly lower the Aβ-induced TUNEL staining even when added 18 hrs post Aβ. With respect to caspase-8, an initiator caspase in the extrinsic pathway, immunoblot assays of brain lysates from 8 month old transgenic AD mice showed that a 2 week oral delivery of hEPN-1 (conjugated to a carrier to deliver it across the blood brain barrier) significantly lowered caspase-8 levels. Finally, an assay of cellular inhibitors of apoptosis (cIAP) showed a significant increase in their cellular levels in SHSY

cells, and in transgenic AD mice treated with hEPN-1, showing for the first time that hEPN-1 may aid cell survival by upregulating proteins known to directly bind specific caspases to block their activity leading to their degradation. The cIAP upregulation occurred in the presence or absence of Aβ, indicating that hEPN-1 likely does not block cell death by directly interfering with the interaction of Aβ with its cell surface receptors, but instead hEPN-1 may activate an independent cell survival signal transduction pathway in neuronal cells.

TABLE OF CONTENTS

LIST OF FIGURES

LIST OF TABLES

ACKNOWLEDGEMENTS

I would first like to thank my advisor, Dr. David Adams. He has been an amazing source of inspiration and motivation throughout my Masters program. He has helped enhance my critical thinking abilities and helped me grow as a scientist. Dr. Adams' excitement when talking about Alzheimer's disease has been extremely infectious and has kept my frustrations as a scientist at bay. In the past two years I have immensely grown as a scientist, and I consider myself extremely fortunate to have had the opportunity to work in Dr. Adams' lab.

Next, I would also like to thank my committee members, Dr. Dan Gibson and Dr. Elizabeth Ryber. Both have been extremely supportive throughout my project and their advice has been greatly appreciated.

Finally, I would like to thank my parents for always being there for me and supporting me in whatever I've wanted to do. I wouldn't be here were it not for their constant encouragement and unconditional love.

BACKGROUND

Alzheimer's disease (AD) is the most prevalent neurodegenerative disease worldwide, with as many as 20 million people affected. In the U.S., the current 5.3 million cases are expected to increase to approximately 7.7 million by 2030, and to between 11-16 million by 2050. AD is the 6th leading cause of death in America, and every 70 seconds an individual develops the disease (Alzheimer's Association, 2009). Currently, there is no cure for AD, and FDA-approved drugs only indirectly treat the symptoms, not the underlying neurodegeneration.

Alzheimer's Disease Mechanism

Alzheimer's pathology consists of two main hallmark lesions: senile plaques and neurofibrillary tangles (NFT) (**Figure-1**). Senile plaques consist of extracellular aggregates of amyloid-beta (Aβ), while NFT's result from the intracellular accumulation of hyper-phosphorylated tau protein.

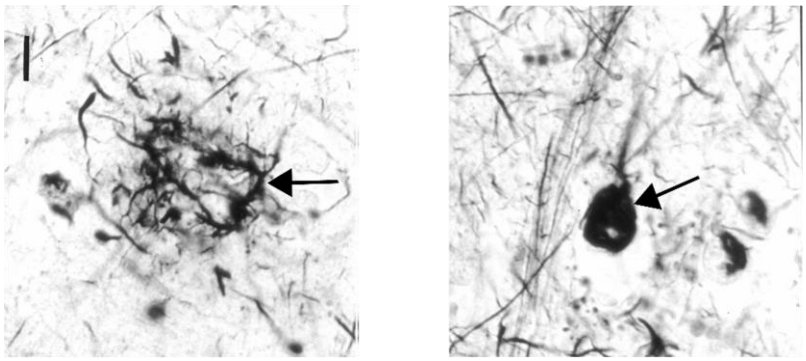

Figure-1: The Two Main Hallmark Lesions of AD. Left Panel: Extracellular senile plaques caused by amyloid-β aggregates. **Right Panel:** Intracellular neurofibrillary tangles (NFT) caused by hyper-phosphorylated tau aggregates. Arrows denote senile plaques (left) and NFT (right) (Armstrong, 2006).

The exact cellular mechanism of AD is unknown, but the most widely accepted hypothesis is termed the *amyloid cascade hypothesis*, which argues that Aβ is the key initiator of the disease, which activates a series of signal transduction events that culminate in the hyper-phosphorylation of tau protein and cell death (Hardy and Selkoe, 2002; Armstrong, 2006; Goedert and Spillantini, 2006). According to the amyloid cascade hypothesis, the onset of AD is caused by the improper processing of amyloid precursor protein (APP) (**Figure-2**).

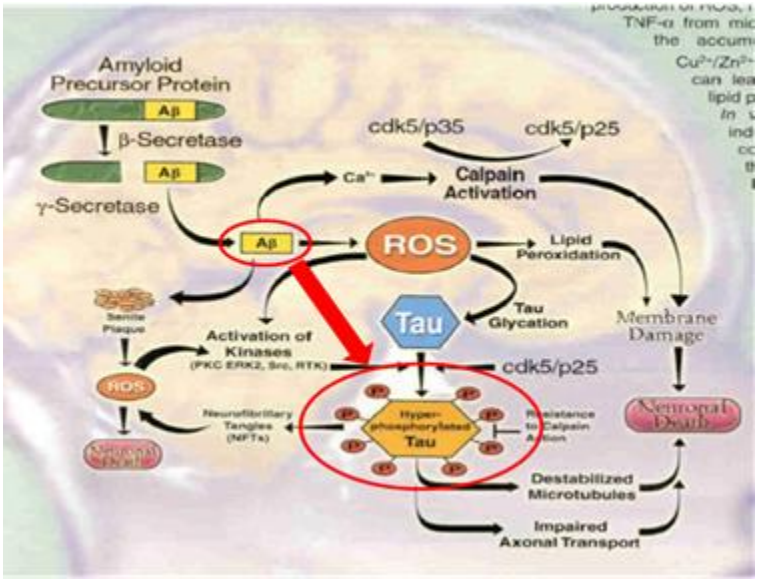

Figure-2: Schematic of Alzheimer's Disease Mechanism. Improper cleavage of APP (green, upper left) on the surface of neuronal and glial cells by beta and gamma secretases leads to the formation of highly neurotoxic Aβ (yellow). The interaction of Aβ with surface receptors such as RAGE leads to a signaling cascade which involves an increase in reactive oxygen species (ROS, orange), Ca^{++} influx, caspase activation, and Tau hyper-phosphorylation (lower center), which finally lead to cell apoptosis (pink). Figure from Calbiochem, 2000.

Aβ has been shown to directly interact with various neuronal cell surface receptors, such as the receptor for advanced glycation end products (RAGE), APP itself, and the NGF receptor p75 (**Figure-3**). Activation of these receptors leads to a series of signaling cascade pathways that result in the formation of reactive oxidative species (ROS), Ca^{++} influx, caspase activation,

and Tau hyper-phosphorylation, all of which ultimately lead to cellular apoptosis (Figures 2 and 3). Tau hyper-phosphorylation destabilizes microtubules, and leads to the formation of neurofibrillary tangles (NTF) (Yaun and Yankner, 2000). The Aβ-RAGE interaction is the best characterized of the Aβ receptors (Yan *et al.*, 1996; Yaun and Yankner, 2000; Yan *et al.*, 2009). The Aβ binding is specific and saturable, and the receptor binding domain has been determined to be a highly potent internal domain $A\beta_{25-35}$ termed the Yankner peptide (discussed below). The Aβ-RAGE interaction occurs on both neurons and microglia. When Aβ binds microglia, the cells release inflammatory tumor necrosis factor-α (TNFα). TNFα binds the TNF-Receptor (TNF-R) on neurons to further increase ROS (Yaun and Yankner, 2000) (**Figure 3**).

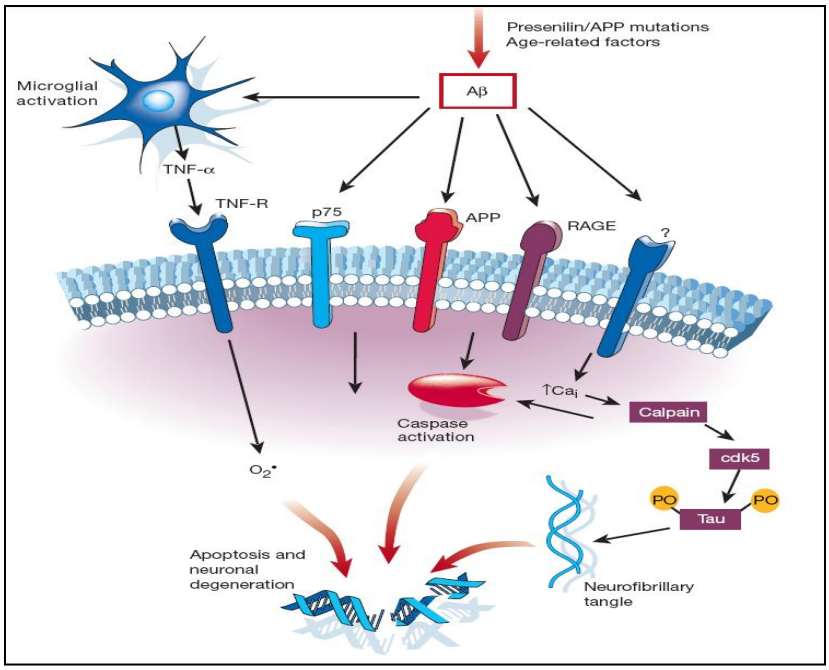

Figure-3: Diagram of Aβ Interaction with Various Neuronal Cell Surface Receptors. Aβ (red square, diagram top) is capable of interacting with receptors like RAGE, APP, and p75 on neurons, or with RAGE on microglia (blue upper left), to initiate TNFα secretion. These interactions initiate signaling cascades that lead to oxidative stress, caspase activation, calcium ion influx, and neurofibrillary tangles, that eventually cause apoptosis (diagram lower center). (Figure from Yuan and Yankner, 2000).

Although historically, the AD field was originally divided into an "amyloid camp" and a "tau camp", with each camp arguing their protein was the molecular key to the disease, we now know that *both* proteins play key roles in neuronal death. Several studies have shown that while Aβ is the key *initiator* of the cell death pathways, hyper-phosphorylated tau is a required end-stage *mediator* of the cell death. Mouse hippocampal cells taken from tau knockout mice and challenged *in vitro* with Aβ do not die, while hippocampal cells taken from mice containing tau and challenged with Aβ die (Rapoport *et al*., 2002). Transgenic AD mice containing a mutant APP gene (modeled after an Indiana early onset AD pedigree, see below) develop AD after about 6 months (Games *et al.*, 1995), but when crossed with tau KO mice, the double mutant offspring containing mutant APP and lacking tau, do not develop AD (Roberson *et al.*, 2007). Thus, in AD, Aβ formation appears to be upstream from tau hyper-phosphorylation.

Although the most important risk factor for AD is age (people over the age of 65 are at higher risk for the disease), some early onset AD cases are inherited. Several genes have been identified that significantly increase AD risk. Inheritance of the apolipoprotein-E (APOE) allele (chromosome-19) (the only currently available commercial AD genetic test) greatly accelerates the formation of Aβ, and increases the risk of sporadic AD about 15-fold (Roberson and Mucke, 2006). In addition, mutations in presenilin -1 or -2 genes (gamma secretase, chromosomes-1 and 14, respectively) (Levy-Lahad *et al.*, 1995; Sherrington *et al.*, 1995; Russo *et al.*, 2000), or in APP itself (chromosome-21) (Levy *et al*., 1990; Chartier-Harlin *et al*., 1991; Goate *et al*., 1991; Murrell *et al*., 1991; Mullan *et al.*, 1992; Tamaoka *et al*., 1994) have all been linked to early onset familial AD (FAD). Each of these mutations results in the increased production of Aβ, and provides support for the amyloid cascade hypothesis (Yuan and Yankner, 2000; Goedert and Spillantini, 2006). Experiments to further enhance our knowledge of Aβ signal transduction

could eventually identify additional mechanistic steps in the Aβ-induced cell death pathway and provide targets for blocking cell death.

The Yankner Peptide

The Yanker peptide was discovered in 1990 by Bruce Yankner of Harvard University (Yankner *et al*., 1990). This peptide is an 11 amino acid derivative ($A\beta_{25-35}$) of full length $A\beta_{1-42}$. $A\beta_{25-35}$ represents the minimal neurotoxic portion of $A\beta_{1-42}$ (Yankner *et al.*, 1990), and is the minimal RAGE receptor-binding domain (Yan *et al*., 1996). $A\beta_{25-35}$ is frequently used for *in vitro* experiments to mimic AD in cultured human SHSY cells, because it is shorter and cheaper to manufacture than full length $A\beta_{1-42}$, yet it appears to be its functional equivalent. Therefore, in our lab, we use $A\beta_{25-35}$ to mimic AD in cultured cells.

General Role of Caspases in Cell Death

Apoptosis is a highly conserved programmed form of cell death. This process plays a vital role in development, and helps maintain homeostasis (Thornberry and Lazebnic, 1998; Shi, 2002; Fan *et al.*, 2005). Suppression or stimulation of this process can lead to acute pathological disorders. For example, suppression of apoptosis can lead to autoimmune diseases, while stimulation can lead to neurological disorders (Yaun and Yankner, 2000; Shi, 2002).

Apoptosis is regulated by caspases. Caspases are aspartate-specific cysteine proteases that cleave substrate proteins after an Asp residue. Caspases are synthesized initially as inactive pro-caspases, and remain inactive until cleaved. Two main pathways lead to the activation of caspases, the *extrinsic* pathway and the *intrinsic* pathway (**Figure-4**). In the *extrinsic* pathway, cell surface death receptors engage death ligands, and the interaction activates intracellular caspases. Early stage caspases in this process are termed *initiator* caspases, which include

caspases-2, -8, and 10. The initiator caspases activate downstream *effector* caspases, which include caspases-3, -6, and -7. Activation of the effector caspases ultimately leads to apoptosis (Thornberry and Lazebnic, 1998; Shi, 2002; Shiozaki and Shi, 2004; Fuentes-Prior and Salvesen, 2004; Fan *et al.*, 2005).

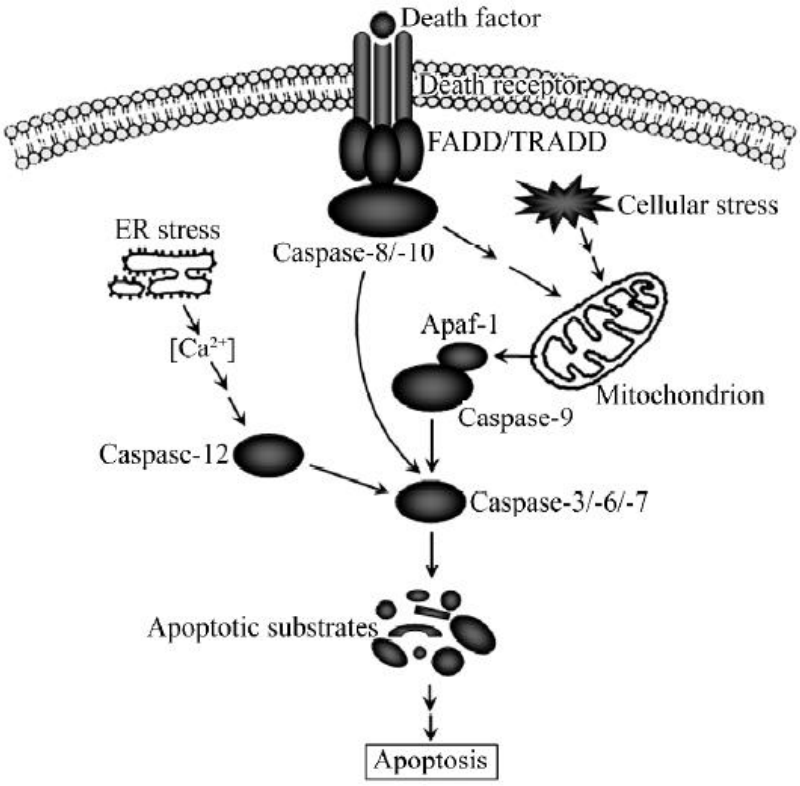

Figure-4: Schematic of Caspase Activation Pathways. The *extrinsic* pathway is activated when a death ligand binds a death receptor (diagam upper), which activates initiator caspases-8 or -10 (upper center). Activation of initiator caspases leads to the activation of effector caspases-3, -6 and -7 (diagram center), which leads to apoptosis (lower diagram). The *intrinsic* pathway is activated by stress to the mitochondria or ER, which activates caspase -9 or -12, respectively (diagram center), which leads to further activation of the effector caspases. (Figure from Fan *et al.*, 2005).

The *intrinsic* caspase pathway is activated when stress is caused to either the mitochondria or ER, which activates caspases-9 or -12, respectively. Activation of the stress caspases results in further activation of the effector caspases. Cellular stresses that activate the

intrinsic pathway include DNA damage, UV radiation, or chemotherapy. These types of stress open the mitochondrial membrane releasing the matrix enzyme cytochrome c (Cyto-c) into the cytosol (**Figure-5**). Cyto-c becomes incorporated into an apoptosome structure that contains two other proteins apoptotic protease activation factor-1 (Apaf-1) and caspase-9. The apoptosome then activates effector caspases -3 and -7, which leads to apoptosis (Green and Reed, 1998; Fan *et al.*, 2005). Activated caspase-3 can also further activate caspase-9 in a positive activation loop (Fan *et al.*, 2005).

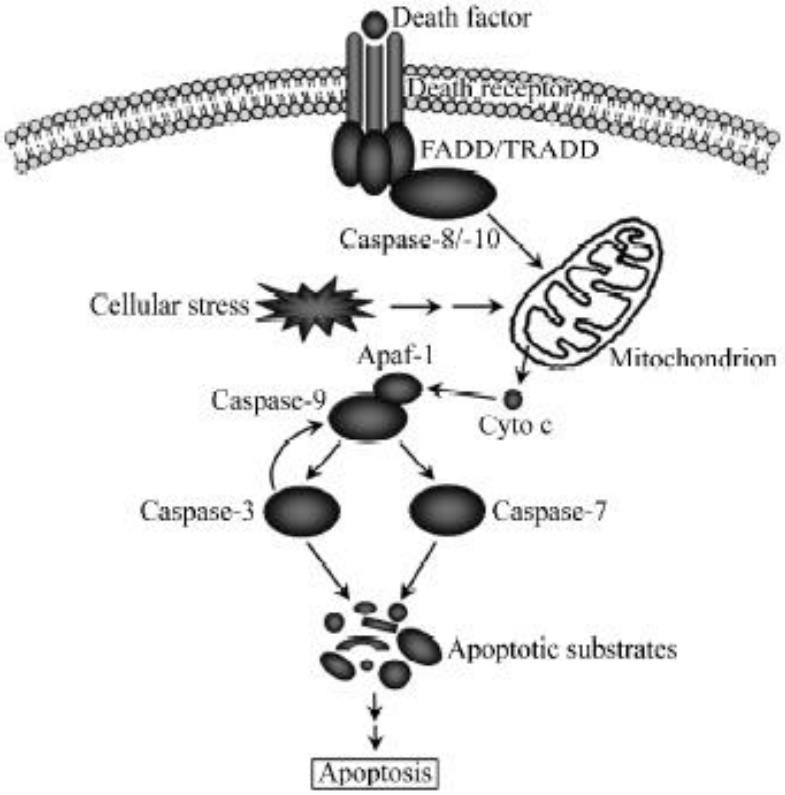

Figure-5: Schematic of the Caspase-9 Stress Activation Pathway. Cellular stress causes the mitochondria to release cytochrome-c (Cyto-c) into the cytosol. Cyto-c causes the activation of apoptotic protease activation factor-1 (Apaf-1) which forms an activating complex with caspase-9. Caspase-9 activates effector caspases -3 and -7, which leads to apoptosis (Figure from Fan *et al.*, 2005).

Regulation of Apoptosis

The caspase apoptotic pathway is regulated by inhibitors of apoptosis (IAP's). These proteins directly bind and inhibit several key caspases. IAP's are a highly conserved family of anti-apoptotic proteins, first discovered in baculovirus genomes (Crook *et al.*, 1993). Since then, IAP homologs have been identified in yeast, nematodes, flies, and mammals, including humans. IAP family members are characterized by the presence of one or more baculoviral IAP repeat (BIR) motifs, and a carboxy-terminal RING finger (Deveraux and Reed, 1999; Salvesen and Duckett, 2002; Liston *et al.*, 2003; Shiozaki and Shi, 2004; Srinivasula and Ashwell, 2008).

Human IAP homologs, cellular IAP1 (cIAP1) and cellular IAP2 (cIAP2) have three BIR motifs and one RING finger (Rothe *et al.*, 1995; Duckett *et al.*, 1996; Uren *et al.*, 1996). The functions of the BIR domains are to bind and inhibit specific caspases. The first BIR domain has not been shown to bind any caspase, but the second BIR (BIR2) domain functions to inhibit caspase -3 and -7, while the third BIR (BIR3) domain functions to inhibit caspase-9 (**Figure-6**) (Roy *et al.*, 1997; Takahashi *et al*., 1998; Bratton *et al*., 2001). The RING fingers in cIAP1 and cIAP2 function in auto-ubiquitylation, a negative IAP regulation pathway that degrades IAPs (Yang *et al.*, 2000).

Smac (second mitochondria-derived activator of caspase) (the second one discovered after Cyto-c) is a negative regulator of IAP. Smac is released from the mitochondria upon apoptotic stimuli, and binds to the BIR domain of cIAP to inactivate the IAP (Figure 6). The Smac/IAP binding is believed to unfold the cIAP molecule to expose the RING finger to cause auto-ubiquitylation which degrades the IAP (Du *et al.*, 2000; Vaux and Silke, 2005; Yang *et al.*, 2000; Yang and Du, 2004). Smac is capable of binding to both BIR2 and BIR3, thereby

preventing IAP from binding caspases-3, -7 and -9. Over-expression of IAPs has been shown to override IAP/Smac binding to allow caspase inhibition (Hunter *et al.*, 2007).

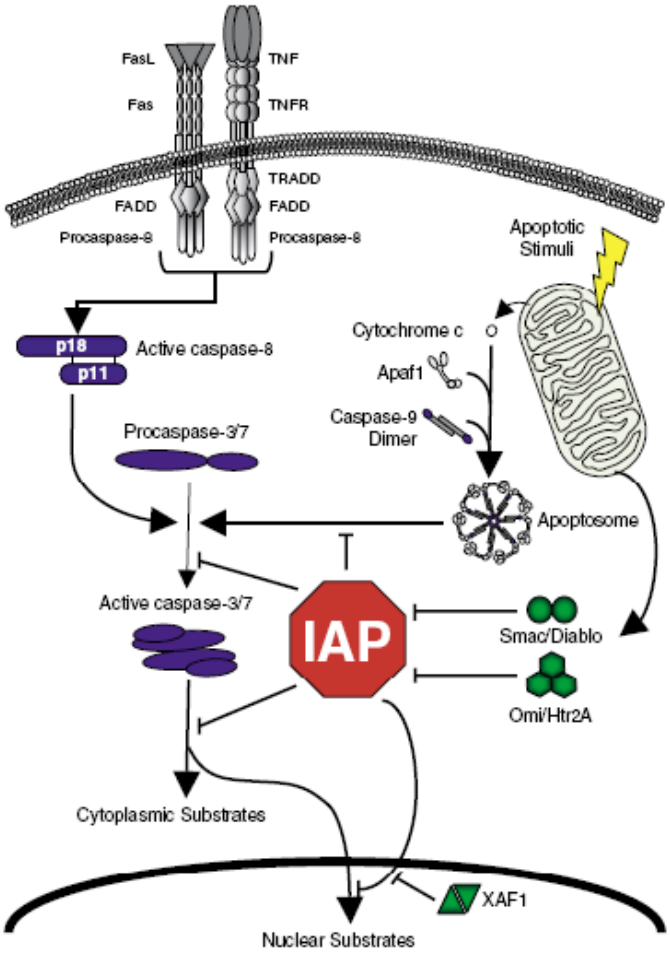

Figure-6: Schematic of the Role of IAP in Blocking Apoptosis. IAP's (red, diagram center) inhibit both the intrinsic caspase-9, and extrinsic caspases-3 and -7. Smac (green, diagram right) acts as a negative regulator of IAP (Figure from Liston *et al.*, 2003).

Because cIAPs have been shown to be key regulators of apoptosis in some systems, this thesis investigated whether they are involved in the blockage of neuronal cell death that our laboratory has observed with some neurotrophic factor treatments (discussed below). However,

any therapeutic activation of IAP's to block cell death must be cautious because cIAP's (and other IAP family members) can act as oncogenes by permanently suppressing cell death (Zender *et al.*, 2006; Hunter *et al.*, 2007). IAP's are also believed to have significant roles in cell division, morphogenesis, heavy metal homeostatsis, NF-$_K$B activation, and MAP kinase signaling (Liston *et al.*, 2003; Srinivasula and Ashwell, 2008). Thus, if an AD therapeutic agent is found to activate IAP to block neuronal cell death, it will also be important to assay for uncontrolled cell division and inflammation.

Current and Future Alzheimer's Therapies

Currently, there is no known cure for AD; however, five FDA approved drugs are sometimes used in an attempt to treat mild to moderate symptoms. The five currently approved AD drugs are (alternative name and approval year in parentheses): Cognex® (Tacrine, 1993), Aricept® (Donepezil, 1996), Exelon® (Rivastigmine, 2000), Razadyne® (Galantamine, 2001), and Namenda® (Memantine, 2003). The first four approved drugs are acetylcholinesterase inhibitors which decrease the degradation of acetylcholine neurotransmitter. Razadyne also helps boost acetylcholine production. Namenda antagonizes the NMDA receptor by blocking excitotoxic glutamate. Unfortunately, these drugs only treat the symptoms of AD, and do not block the underlying neurodegeneration. In addition, their effects, if any, are short lived, and the patient eventually develops desensitization.

Future AD therapies likely will need a three pronged approach, based on our current knowledge of the mechanism of Aβ-induced neurodegeneration: 1) blockage of toxic Aβ formation by inhibiting beta or gamma secretases, 2) removing existing toxic Aβ, and 3) blocking cell death or reversing neurodegeneration. With respect to prong-1, six γ-secretase

inhibitors are currently in clinical trials, and preliminary data indicate three of the six have reduced Aβ levels in patient cerebrospinal fluid (Imbimbo, 2008). With respect to β-secretase, a membrane targeting approach (the site of secretase activity) using a sterol-linked β-secretase inhibitor, was found to reduce APP cleavage by 80% in cultured cells and in transgenic AD mice (Rajendran *et al.*, 2008). Hence, both β and γ-secretase inhibitors could potentially hinder Aβ formation.

With respect to prong-2 (removing existing Aβ), Elan Pharmaceuticals Inc. has performed two Phase III clinical trials with a vaccine containing antibodies against Aβ to remove existing Aβ from the brain. The initial vaccine tested in mice (Schenk *et al.,* 1999) was performed on the AD mouse model developed in part in our laboratory (Games *et al.,* 1995), and the mice showed significant plaque reduction and behavioral improvements. With respect to human clinical trials, although a small percentage of patients in the first trial showed evidence of brain inflammation (likely due to cross reactivity of the antibodies with endogenous APP) (Hardy and Selkoe, 2002), no patients showed similar symptoms in the second clinical trial using a second generation vaccine designed against a different region of Aβ. Unfortunately, the patients tested did not show significant behavioral improvements, thus the use of only a one-prong approach likely will not successfully treat AD.

With respect to prong-3 (blocking or reversing cell death), Dimebon® is an orally active drug used in Russia as an antihistamine since 1983. In animal studies, it has been shown to inhibit brain cell death, so it may have applications for AD, Parkinson's disease, or Huntington's disease (Lermontova *et al*., 2000; Bachurin *et al*., 2001; New York Times, 2007). In a Phase-III-equivalent trial in Russia, Dimebon showed cognitive improvement in patients with mild to moderate AD (Doody *et al.,* 2008). Dimebon appears to inhibit L-type calcium channels and

modulate the action of AMPA and NMDA glutamate receptors (Grigorev *et al*., 2003). Unfortunately, it may also block other receptors including α-adrenergic receptors and serotonin receptors, and may also *increase* Aβ levels in the brain, so the testing of this drug continues (Alzheimer's Association, 2009). Our laboratory is currently testing the use of neurotrophic factors, proteins that aid neuronal survival and growth, as potential AD therapeutics (see below).

Neurotrophic Factors and Alzheimer's Disease

Neurotrophic factors (NTFs) are proteins that normally function in brain development to stimulate neuronal growth and regeneration (Lindsay *et al*., 1994), but evidence also shows their levels increase in the brain following injury (Connor and Dragunow, 1998; Ferrer *et al.*, 1998). Thus, NTFs have been investigated as possible therapeutics for neural disorders (Barinaga, 1994; Tuszynski and Gage, 1994; Shen *et al.*, 1997; Hefti, 1997; Yu and Silva, 2008; Zuccato and Cattaneo, 2009). Our lab is interested in testing NTFs as potential AD therapeutics. Ependymins (EPNs) are NTFs initially discovered in the *zona ependymal* cells of goldfish brains, from which their name is derived (Benowitz and Shashoua, 1997). Since their initial discovery, the Adams and Shashoua labs have identified ependymins in a variety of organsims (Adams and Shashoua, 1994; Adams *et al*., 1996), and ependymins have also been identified in mice, monkeys, and humans (Apostolopoulos *et al*., 2001).

With respect to using ependymins as therapeutics, full length ependymins (approximately 215 amino acids long) cannot cross the blood brain barrier (BBB) when administered i.v., i.p. or by oral gavage, therefore the Adams/Shashoua labs have adopted an approach that utilizes shorter synthetic versions of EPN capable of crossing the BBB. Using this peptide approach, our labs showed that treatment of cultured neuronal cells with EPN-derived peptides stimulates a

MAPK pathway to activate transcription factor AP-1, a key regulator of neuronal survival and long term potentiation (Adams *et al.*, 2003). EPN-derived peptides were also found to be neuroprotective in *in vitro* and *in vivo* rat models of cerebral ischemia (Shashoua *et al.*, 2003), and were found to activate key anti-oxidative enzymes (SOD, catalase, and glutathionine peroxidase) to help alleviate cellular oxidative stress (Shashoua *et al.*, 2004).

With respect to using EPN peptides as AD therapeutics, previous work in our lab has shown that treatment of cultured human SHSY neuronal cells with $A\beta_{25-35}$ decreases cell survival, while the addition of human EPN-1 peptide (hEPN-1) restores survival (Stovall, 2006). A subsequent thesis showed that the $A\beta_{25-35}$ treatment of SHSY cells increases cellular levels of caspases-2 and -3, while the addition of hEPN-1 significantly lowers both levels (Kapoor, 2007). Enzyme activity measurements for caspase-3 showed similar data, with $A\beta_{25-35}$ strongly increasing activity, and hEPN-1 reversing the increase (Kapoor, 2007). In transgenic AD mice, brain levels of caspase-7 increased over time (as the levels of Aβ increased), and the caspase-7 increase was blocked in AD mice treated orally for 2 weeks with hEPN-1 peptide (Ronayne, 2008). In addition, treating SHSY cells with Aβ was found to increase TUNEL staining, an assay for DNA fragmentation (a hallmark end stage of apoptosis, and a different apoptotic marker than caspase activation). And treatment with hEPN-1 simultaneously with the Aβ, or 6 hrs post Aβ, significantly lowered the Aβ-induced TUNEL signal (Ronayne, 2008). Thus, our lab's previous data show that Aβ activates key members of the *extrinsic* caspase cell death pathway in cultured human neuronal cells and in transgenic mouse brains, and that hEPN-1 treatment helps counteract the effects of Aβ.

THESIS PURPOSE

Previous work in our laboratory showed that cultured human SHSY neuronal cells treated with $A\beta_{25-35}$ decreases cell survival, while the simultaneous or post-addition of hEPN-1 as an AD therapeutic can completely or partially, respectively, restore cell survival (Stovall, 2006). With respect to the mechanism of cell death, treatment of SHSY cells with $A\beta_{25-35}$ increases the cellular levels of *extrinsic* pathway initiator caspase-2 and effector caspase-3, while the simultaneous or post-addition of hEPN-1 significantly lowers their levels (Kapoor, 2007). In transgenic AD mice, brain levels of effector caspase-7 increase over time (as the levels of Aβ increase), and the caspase-7 increase was blocked in AD mice treated orally for 2 weeks with hEPN-1 peptide (Ronayne, 2008). And hEPN-1 treatment of of SHSY cells, simultaneously with Aβ, or 6 hr post Aβ, can block Aβ-induced TUNEL staining for DNA fragmentation, a key end stage marker of apoptosis (Ronayne, 2008). Thus, Aβ appears to activate the *extrinsic* apoptotic pathway, both *in vitro* and *in vivo*, and hEPN-1 can reverse the activation. This thesis extends these findings by analyzing another key member of the *extrinsic* pathway, initiator caspase-8, which was not previously studied. To determine whether activation of the *extrinsic* pathway also activates the *intrinsic* apoptotic pathway, the thesis also analyzes a key initiator caspase in this pathway, caspase-9. In addition, in an attempt to begin identifying the mechanism of hEPN-1 blockage of the extrinsic pathway and cell death, the thesis examines the cellular levels of a cellular inhibitor of apoptosis (cIAP). Finally, a portion of this thesis extended our earlier TUNEL experiments to attempt to block Aβ-induced TUNEL staining when adding hEPN-1 to cultures at time periods longer than 6 hours post-Aβ. Thus, the goal of this project is to analyze

additional members of the caspase family than studied previously, and to analyze inhibitors of caspases, as well as to extend our nuclear DNA fragmentation experiments.

MATERIALS AND METHODS

Human SH-SY5Y Neuroblastoma Cell Culture

Human SH-SY5Y (SHSY) neuroblastoma cells were purchased from ATCC (CRL-2266), and the vials were stored in liquid nitrogen. Cell culture medium was made using a 500 mL bottle of DMEM/F-12 (1:1 ratio of Dulbecco's Modified Eagle's Medium to Ham's F12 Nutrient Mixture; ATCC #30-2006), to which was added 50 mL of FBS (Fetal Bovine Serum; ATCC #30-2020) (to make a final concentration of 10%) and 0.275 mL of 10 mg/mL gentamicin (Invitrogen #15710-064) (to make a final concentration of 5 µg/mL). The mixture was filter sterilized using a 0.2 µm filtration flask, and stored at 4˚C.

A vial containing frozen cells was quick-thawed for 30 seconds in a 37˚C water bath, and then immediately transferred to a 15mL conical tube. 10 mL of pre-warmed culture medium was slowly added to the tube, and the cell suspension was centrifuged for 5 minutes at 100x g to remove the DMSO from the freezing medium. The medium was aspirated, and the cell pellet was resuspended in 4 mL of pre-warmed culture medium. The 4 mL suspension was transferred to a T-25 flask, and the flask was placed in a 37˚C humidified incubator with an atmosphere of 5% CO_2.

Flasks were split 1:2 every 2-4 days, or when they reached 80% confluency, using trypsinization. Spent medium was siphoned to waste, then 1 mL of 0.25% Trypsin-EDTA (Invitrogen #25200-106) was added. The flask was incubated at room temperature for 30 seconds to 1 minute until the cells became loose, then the cells were immediately transferred to a 15ml plastic tube and centrifuged at 5,000 rpm for 5 minutes to pellet the cells. 8 mL of pre-warmed medium was added to the cell pellet, and the cells were resuspended. The suspension

was transferred to two T-25 flasks, 4 ml per flask. Routine feeding was performed every other day by aspirating the spent medium and adding 4 mL of fresh medium.

Yankner Peptide

Yankner peptide ($A\beta_{25-32}$) was purchased from CS Bio Company (Menlo Park, CA) in a dry powder form, and stored at -20˚C. In order to prepare a working stock, 1 mg (943 nmol) of the powder was mixed with 943 µl of 1 mM sodium bicarbonate ($NaHCO_3$) to make a final concentration of 1.0 mM. The solution was then sonicated for 30 seconds to dissolve the powder. The solution was stored at -20°C. In order to produce a neurotoxic effect, the dissolved peptide was used at a 1:50 dilution, to make a final concentration of 20 µM. For example, 80 µl was added to 4 ml medium in a T-25 flask, or 20 µl was added to 1 ml of medium in a 24-well microtiter well.

hEPN-1 Peptide

The human ependymin-1 peptide (hEPN-1) was acquired from Biotherapeutix, Inc. (Brookline, MA) in a dry powder form, and stored at -20˚C. In order to prepare a working stock, 1 mg of powder (MW varied depending on the particular salt of that batch) was mixed with an appropriate volume of serum-free DMEM to prepare a stock concentration of 3.75 mM. For experimental purposes, the peptide was used at a 1:25 dilution, to make at a final concentration of 150 µM. For example, 160 µl was added to 4 ml medium in a T-25 flask, or 40 µl was added to 1 ml of medium in a 24-well microtiter well.

Cell Plating Experiments

In order to plate cells for experimental purposes, SHSY cells were plated in T-25 flasks to give ~80% confluency after 72 hrs. To obtain cell counts, cells were stained for trypan blue exclusion, and counted in a hemocytometer. Viable cells were observed as a brownish color with a blue halo (blue exclusion), while non-viable cells stained completely blue. Cell counts were obtained using the following formula:

> Number of cells/mL = (Number of cells counted/ Number of primary squares counted) x the dilution factor (usually 2) x 10^4

To determine the cell number to give ~80% confluency (which varied depending on the culture vitality, and the number of passages), cells were plated in 24-well microtitier plates at various concentrations (between 1.0 to 6.0 x 10^5 cells/mL) and grown for 72 hours. Usually, the concentration that produced ~80% confluency after 72 hrs was 5 x 10^5 cells/mL.

Cells were plated in T-25 flasks in a total volume of 4 mL (or 1 ml in a 24-well microtiter plate) and allowed to settle for 24 hours before insult (Yankner peptide) or therapy (hEPN-1) peptides were added. For time-course experiments, cells were incubated with Yankner peptide (for caspase experiments) or hEPN-1 (for cIAP experiments) for various lengths of time (0, 24, 48 and 72 hrs) to determine the optimum effects. Whole cell extracts were then prepared (see below), and caspase or cIAP assays were performed. Once the optimum time point was determined for a particular assay, subsequent flasks were simultaneously treated with Yankner and hEPN-1, then incubated for the optimum time.

Preparation of Whole Cell Extracts

Following incubation with the appropriate peptide, cells were harvested from a flask by using a plastic cell scraper. The spent medium was removed by centrifugation, and the cells were washed 1X in PBS in a 1.5ml eppendorf tube. To the final cell pellet was added 200 µl of Lysis Buffer (20 mM HEPES pH 7.9, 10 mM KCl, 300 mM NaCl, 1 mM $MgCl_2$, 0.1% Triton X-100, 20% glycerol. 0.5 mM fresh DTT, 0.5 mM fresh PMSF). The tubes were vortexed to mix, and then placed on ice for 10 minutes to swell the cells and complete the cell lysis (tubes were periodically vortexed during this incubation). Resuspension of the lysate using a micropipette was not required for cell lysis. Following the lysis, lysates were centrifuged in a microcentrifuge at high speed for 5 minutes at 4°C for clarification. Cleared supernatants were stored at -80°C. The total protein content of each lysate was determined using a Bradford Assay (Coomassie Protein Reagent, Pierce #23200) compared to a BSA standard curve.

Western Blots

Protein samples were electrophoresed on 10% polyacrylamide-SDS gels, as described in Ronayne (2008), using various protein loads (see figure legends). The separated proteins were blotted to nitrocellulose membrane using a transblot apparatus as previously described. Membrane blocking was performed in freshly prepared Blocking Solution (1X PBS pH 7.5, 1% casein, 0.2% tween-20) overnight at 4°C. Primary antibody incubations were performed in a heat-sealed plastic bag for 2 hrs at 25°C, using 2-3 mL of Blocking Solution (depending on the size of the membrane) and primary antibody as shown in **Table I**. Secondary antibody incubations were performed for 2 hrs at 25°C in 10 mL of Blocking Solution (20-25 mL for larger blots) containing a final concentration of 0.4 µg/mL of goat anti-rabbit-HRP (Pierce

#31460), or 0.4 µg/mL of goat anti-mouse-HRP (Pierce #31430). Chemiluminescent detection was performed using equal volumes of Luminol-Enhancer and Stable Peroxide (Pierce #34080). Film development was performed on an automatic film processor.

Table 1. Primary Antibody Concentrations.

Antibody	Vendor	Host	Specificity	Stock Concentration	Final Concentration
Caspase-3	Imgenex (IMG-144A)	Mouse	Human, Mouse	500 µg/mL	2 µg/mL (i.e. 4 µl/mL)
Caspase-8	Imgenex (IMG-5561)	Rabbit	Human, Rat, Mouse	1000 µg/mL	1 µg/mL (i.e. 1 µl/mL)
Caspase-9	Abcam (ab-2013)	Rabbit	Human, Rat, Mouse	500 µg/mL	1.5 µg/mL (i.e. 3 µl/mL)
cIAP-1	Millipore (AB 3614)	Rabbit	Human, Rat, Mouse	200 µg/mL	1 µg/mL (i.e. 5 µl/mL)
cIAP-1/2	Imgenex (IMG-5444-2)	Rabbit	Human, Mouse	1000 µg/mL	2 µg/mL (i.e. 2 µl/mL)
β-Tubulin	Imgenex (IMG-5810A)	Rabbit	Bovine, Chicken, Dog, Human, Monkey, Mouse, Rat, Xenopus	500 µg/mL	1 µg/mL (i.e. 2 µl/mL)

Immunoprecipitations

In order to remove proteins in the lysates that bind secondary antibody, immuno-precipitation experiments were performed using secondary antibody. Lysate volumes equivalent to 10 immunoblots were mixed with PBS in 0.5ml eppendorf tubes to make a volume of 100 µl. 5.0 µl of secondary antibody (see Western blot section) was added to each sample, and the tubes were incubated for 2 hours at room temperature on a shaker. After the antibody incubation, 100

µl of Protein-A/Acrylic beads (Sigma # P-1052) were added to each sample, and the tubes were incubated for 1 hr at room temperature on a shaker. Each sample was then microcentrifuged for 5 minutes at high speed to pellet the beads. The supernatant was carefully aliquoted into new 0.5ml eppendorf tubes, being careful not to include any beads. Then a western blot was performed as described above, using 10 µl of cleared supernatant.

In Vivo Alzheimer's Mouse Experiments

Double mutant Alzheimer's mice used in this thesis were purchased by Dr. Cindy Lemere at the Brigham and Women's Hospital (Boston) from The Jackson Laboratory (Bar Harbor, ME, Stock #004462). The mice contain an APPswe mutation that mimics an early onset Swedish family, showing accelerated Aβ production, and a PSEN1dE9 mutation within the presenilin-1 gene that results in an elevation of γ-secretase activity which also causes overproduction of $A\beta_{1-42}$. The Jackson Laboratory maintained the mice as hemizygotes with the transgene inserted at a single locus, and it was shown by other labs to be expressed in the neurons of the central nervous system. The first Aβ deposits were observed at approximately 5-6 months, and they became pronounced at 11 months of age (Jankowsky *et al.*, 2001; 2004). Behaviorally, these mutants show learning impairments (Reiserer *et al.*, 2007). 50% of the offspring mice are wild-type (containing no transgenes), and these mice were used as controls.

In Dr. Lemere's lab, the mice were aged to 8 months, then divided into four experimental groups (3 mice per group): wild type (WT) vehicle, WT hEPN-1, Alzheimer's (Alz) Vehicle, and Alz hEPN-1. The vehicle used was dH_2O. The hEPN-1 used in this particular experiment was covalently linked to DHA carrier by BioTherapeutix to allow penetration across the blood brain barrier. The peptide was administered by *p.o.* dosing (oral gavage) to the mice at a dose of

0.2 mL of 30 mg/kg, twice a day for 2 weeks. After 2 weeks, the mice were anesthetized using CO_2 then sacrificed by decapitation. The brains were perfused with PBS to remove blood, then stored at -80˚C, until shipment to WPI on dry ice.

Brain Homogenization

Materials used during this process at WPI were kept on ice as much as possible. A 1 mg portion of brain cortex was added to 1.0 mL of Lysis Buffer (see Preparation of Whole Cell Lysates section), in a 1.0 mL glass dounce homogenizer. The tissue was disrupted by 10 up-and-down strokes, then the homogenate was placed in a 1.5mL eppendorf tube and microcentrifuged for 5 minutes at high speed at 4˚C to pellet cell debris. The cleared supernatant was collected and stored at -80˚C. Protein concentration was determined using a Bradford assay, as described in the Whole Cell Lysates section.

TUNEL Assay

Terminal-deoxynucleotidyl Transferase Biotin-dUTP Nick End Labeling (TUNEL) assays were performed to quantitate the level of fragmented DNA in various cell cultures at different time points. Cells were plated on 24-well microtiter plates at a concentration of 2.5 x 10^4 cells per mL, then placed in the culture incubator for ~24 hrs before the addition of peptides to final concentrations as listed in the peptide subsections. Following Aβ addition, hEPN-1 was added either simultaneously or post-insult at 9, 12 or 18 hrs. After the addition of peptides, the cells were incubated for ~24 hrs before collection.

The cells were harvested via trypsinization (see SHSY culture section) using approximately 300 µL of trypsin-EDTA solution. 1 mL of culture medium was added to the

300 µL to stop the reaction, and the cell suspension was transferred to 1.5mL Eppendorf tubes. Tubes were spun for 5 minutes at 7,000 rpm in a microcentrifuge to pellet the cells. The cell pellet was washed once in 50 µL of 1X PBS, and centrifuged for 1 minute at 7,000 rpm. The washed pellet was then resuspended in 20 µL of 1X PBS, and the entire 20 µL was added to the center of a previously prepared poly-L-lysine (VWR #IC15017725) coated microscope slide, and air-dried in the tissue culture hood for 20-25 minutes. Microscope slides were pre-coated with poly-L-lysine by adding 20 µL of a 1:10 dilution of 0.1 mg/mL poly-L-lysine in dH_2O at the end of a slide and distributing it in a thin layer using the edge of another microscope slide. Immediately after the slides were coated, they were air-dried, then rinsed in dH_2O. After the rinse, the slides were air dried again for 30-60 minutes.

After spreading the 20 µL cell suspension on the pre-coated poly-L-lysine slides, cells were fixed by immersing the slides in 10% neutral buffered formalin (VWR #83009-256) in a Coplin jar (Rolle lab) for 25 minutes at room temperature. Slides were then washed twice by immersion in 1X PBS at room temperature for 5 minutes. At this stage in the assay, slides can be stored in 1X PBS at 4˚C overnight, or can be stored longer term in 70% ethanol at -20˚C.

To permeabilize the cells, the slides were immersed in 0.2% Triton X-100 (Sigma), (freshly diluted in 1X PBS) for 5 minutes at room temperature. Slides were washed twice in 1X PBS for 5 minutes at room temperature. Excess liquid was removed from the slides by tapping, after which 100 µL of equilibration buffer (TUNEL Kit, Promega # G-7360) was added to the fixed cell spot for 10 minutes at room temperature. Next, a Kimwipe was used to remove moisture from the slide, then 100 µL of freshly prepared rTdT reaction mix (Promega TUNEL Kit, **Table 2**) was added to the equilibrated cells. Each component of the rTdT reaction mix was thawed on ice and the final reaction mix was kept on ice until use. After adding the 100 µL

reaction mix to each slide, a plastic cover slip (Promega TUNEL Kit) was placed on top of the cells to evenly distribute the reaction mix. The slides were then placed at 37˚C in a humidified chamber (cell culture incubator) for 1 hour to allow the end-labeling reaction to take place.

Table 2. Preparation of rTdT Reaction Mix.

TUNEL Kit Component	Component Volume per Standard Reaction (100 µL per slide)
Equilibration Buffer	98 µl
Biotinylated Nucleotide Mix	1 µl
rTdT Enzyme	1 µl

At the end of 1 hour TdT incubation, the slides were removed from the humidified chamber and the cover slips were removed. The slides were then immersed in 2X SSC (Promega TUNEL Kit; diluted with dH_2O) for 15 minutes at room temperature, to terminate the end labeling reactions. Next, the slides were washed three times in 1X PBS for 5 minutes each at room temperature to remove unincorporated biotinylated-UTP nucleotide. The slides were then immersed in 0.3% hydrogen peroxide (Sigma) (diluted in 1X PBS) for 5 minutes at room temperature to block endogenous peroxidases. The slides were washed 3 times in 1X PBS for 5 minutes each at room temperature, after which the slides were tapped to remove excess liquid.

To develop the reactions, streptavidin-HRP (Promega TUNEL Kit) was diluted 1:500 in PBS, and 100 µL was added to each slide. Slides were incubated for 30 min at room temperature, then washed 3 times by immersion in 1X PBS for 5 minutes at room temperature. Immediately before use, 100 µL of DAB solution was prepared per slide (**Table 3**), and the 100

µL of DAB solution was added to each slide. The slides were incubated for ~10 min at room temperature or until a light brown background appeared. Slides were rinsed several times with dH_2O and then air dried. 1 drop of aqueous mounting medium (VWR #100496-546) was added to each slide, and a cover slip was placed on top. Cover slips were sealed around the edges using clear nail polish, and air dried. Slides were viewed on a Lecia DM LB2 microscope (Gaudette Lab) at 100X magnification (10X objective) using the Leica Application Suite software.

Table 3. Preparation of DAB Reaction Mix.

TUNEL Kit Component	Component Volume per Standard Reaction (100 µL per slide)
dH_2O	95 µL
DAB Substrate 20X buffer	5 µl
DAB 20X chromogen	5 µl
Hydrogen Peroxide	5 µl

Note: The volume in the table is greater than 100 µL, but only 100 µL was added per slide.

Data Analysis

Immunoblots

Developed immunoblot x-ray films were analyzed using Scion Image Software (NIH) to quantitate relative band densities, recorded as optical density (OD). For *in vitro* experiments, all OD values were normalized relative to untreated control samples. For *in vivo* mouse brain extract data, the treated Alz mice were normalized relative to untreated Alz mice. To statistically evaluate immunoblot data, values (as fold changes relative to intra-set controls) were analyzed

using one-way Analysis of Variance (ANOVA) and conservative HSD posthoc analysis, on SPSS software to determine data significance at a 95% confidence level.

Analysis of TUNEL Data

TUNEL data was analyzed visually in three randomly chosen optical fields captured on the microscope using the Leica Application Suite Software (Gaudette lab). Images were then transferred to a powerpoint file where they were divided into quadrants. Stained (medium to dark brown) and unstained (clear to light brown) cells were counted in each quadrant, and these numbers were added to obtain the cell values for each field. Black debris was not incorporated into cell counts. Values obtained for each field were averaged and then converted to percent of cells undergoing apoptosis. To statistically evaluate the TUNEL data, the percent apoptotic cell values were analyzed using ANOVA and HSD posthoc analysis, as described above.

RESULTS

Caspase-9 Experiments

Because previous work in our laboratory demonstrated that treatment of cultured human neuronal SHSY cells with $A\beta_{25-35}$ activates key components of the *extrinsic* caspase apoptotic pathway leading to cell death, we wanted to test whether activation of this extrinsic pathway also activates an *intrinsic* stress caspase pathway. Caspase-9 is a key initiator caspase in the intrinsic mitochondrial stress pathway (discussed in the Background section), so we chose to assay its potential upregulation by Aβ, and its downregulation by hEPN-1. First, an Aβ time-course experiment was performed (**Figure- 7)** to attempt to identify an incubation time where caspase-9 upregulation might be visible.

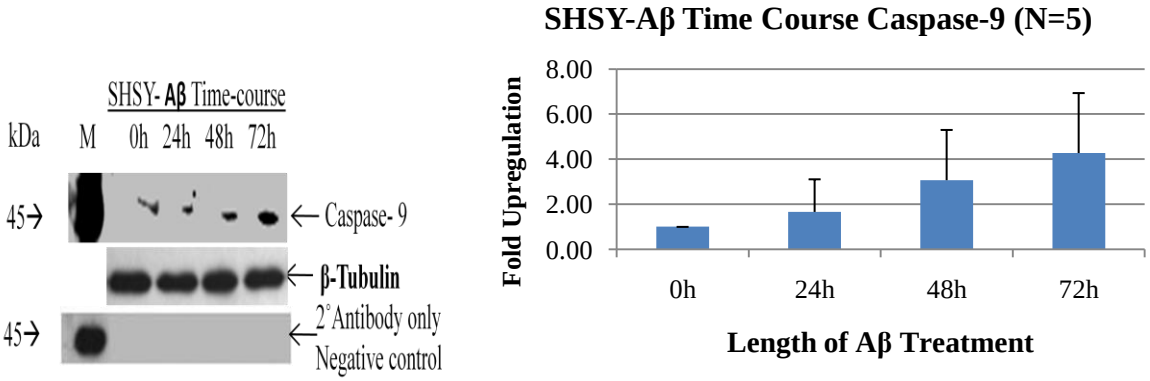

Figure-7: Time-Course of Upregulation of Caspase-9 by Aβ *In Vitro*. Left Panel: The upper blot is a caspase-9 immunoblot using an Abcam antibody that detects caspase-9 at ~45 kDa. "M" denotes a biotinylated size marker. The middle blot is a β-tubulin immunoblot run as a load control. The lower blot is a negative control lacking primary antibody. All blots were run simultaneously using the same 20 µg protein load. **Right Panel:** Quantification of caspase-9 band intensities. Histobars denote the average of 5 independent trials. Error bars denote one standard deviation.

Cells were treated with 20 μM of $A\beta_{25-35}$ (a concentration previously shown in our lab to activate the *extrinsic* pathway and induce cell death within 3 days) for various time points. The results showed a band of the expected 45 kDa size for caspase-9 (upper blot) whose intensity increased above the untreated control at each time point tested (24, 48, and 72 hrs). The β-tubulin load control signal remained unchanged (middle blot). The 45 kDa band was not present in a negative control lacking primary antibody (lower blot), so the band appears to be specific to the primary antibody. The caspase-9 signal was maximal at 72 hrs, approximately 4.3 fold above control levels (N=5) (although the elevation was not statistically significant); therefore, this 72 hr time point was chosen for further analysis with hEPN-1 to determine whether that treatment reduces caspase-9 levels (**Figure-8**).

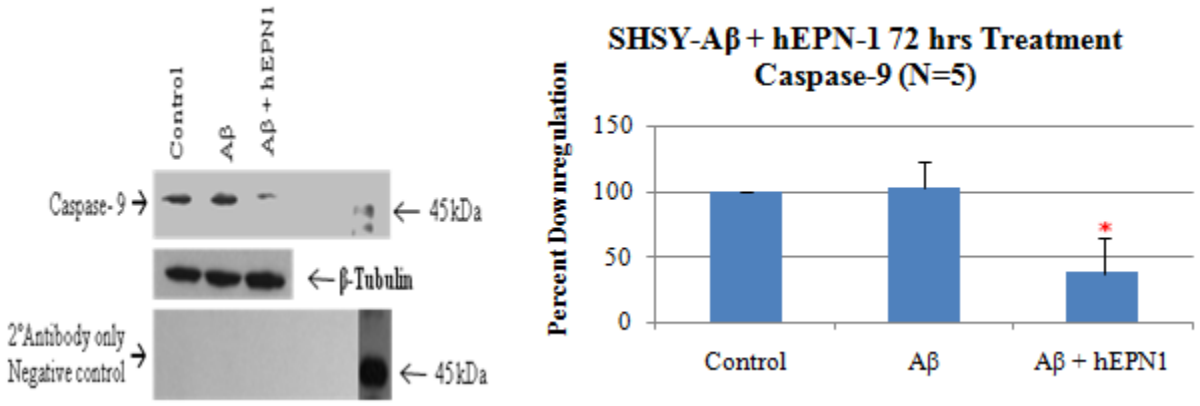

Figure-8: hEPN-1 Treatment of SYSY Cells Reduces Caspase-9 Levels. Left Panel: Upper blot is a caspase-9 immunoblot using an antibody that detects caspase-9 at ~45 kDa. The middle blot is a β-tubulin immunoblot run as a load control. The lower blot is a negative control lacking primary antibody. All blots were run simultaneously with the same 20 μg protein load. **Right Panel:** Quantification of caspase-9 bands. Histobars denote the average of 5 independent trials. Error bars denote one standard deviation. * Indicates significance from control and Aβ at the 95% confidence level using a one way ANOVA followed by HSD post-hoc tests.

In this particular set of experiments (N=5), the caspase-9 signal did not appear to increase with the Aβ treatment (middle histobar), although the increase was very clear in the previous set of experiments. But the experiment did clearly show that simultaneous treatment of the cells with

Aβ + hEPN-1 (right histobar) significantly lowered (95% confidence) the cellular levels of caspase-9.

To determine whether the apparent lack of caspase-9 elevation by Aβ in this particular set of experiments resulted from an inactive batch of Aβ, caspase-3 immunoblots were performed on the lysates (**Figure-9**) since several previous experiments in our lab showed that Aβ elevates the levels of this caspase. The results show that Aβ (middle histobar) significantly (95% confidence using HSD post-hoc tests) increases the levels of caspase-3 relative to untreated cells at, and that simultaneous treatment with hEPN-1 significantly lowers the signal (right histobar). This caspase-3 data validates previous thesis data from our lab (Kapoor, 2007) which was at the LSD level, and indicates the Aβ batch is active.

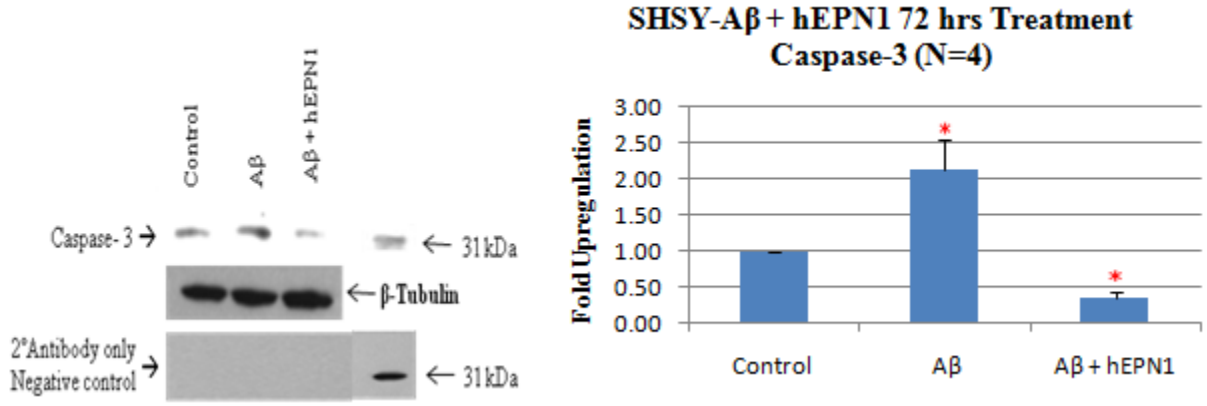

Figure-9: hEPN-1 Reduces Caspase-3 Levels *In Vitro*. Left Panel: Upper blot shows a caspase-3 immunoblot using an antibody that detects caspase-3 at ~31 kDa. The middle blot shows a β-tubulin immunoblot run as a load control. The lower blot is a negative control blot lacking primary antibody. All blots were run simultaneously with the same 20 µg protein load. **Right Panel:** Quantification of caspase-3 bands. Histobars denote average of 4 independent trials. Errors bars represent one standard deviation. * Indicates significant difference from all other groups at the 95% confidence level using a one way ANOVA followed by HSD post-hoc tests.

The data from the caspase-9 experiments indicate it is *inconclusive* whether treatment of SHSY cells with Aβ activates the mitochondrial stress *intrinsic* apoptotic pathway, so more experiments are required to test this. But more importantly, the data clearly show a significant decrease in caspase-9 levels in SHSY cells treated simultaneously with Aβ + hEPN-1; thus, hEPN-1 appears to block both the *extrinsic* apoptotic pathway (previous data for caspase-2) and the *intrinsic* pathway (caspase-9).

TUNEL Assay *In Vitro*

In order to assay apoptosis using an assay other than levels of caspase enzymes, a Terminal-deoxynucleotidyl Transferase Biotin-dUTP Nick End Labeling (TUNEL) assay was performed. This assay quantitates a hallmark endstage of apoptosis, DNA fragmentation, by incorporating a biotinylated nucleotide (dUTP) onto the 3'OH end of fragmented DNA catalyzed by recombinant Deoxynucleotidyl Transferase (rTDT). The incorporated biotinylated dUTP is detected by streptavidin-HRP, and visualized by diaminobenzidine (DAB). Apoptotic cells that contain fragmented DNA stain brown. We began by performing an Aβ time-course to identify an incubation time that might show TUNEL staining (**Figure-10**). Quantitation of the data from one experiment (histoplot) showed that the TUNEL staining clearly increased with the time of Aβ incubation, with all time points tested showing higher staining than the untreated 0 Hr control. The staining was highest at the longest time tested (18 hr), with a 23-fold upregulation relative to control.

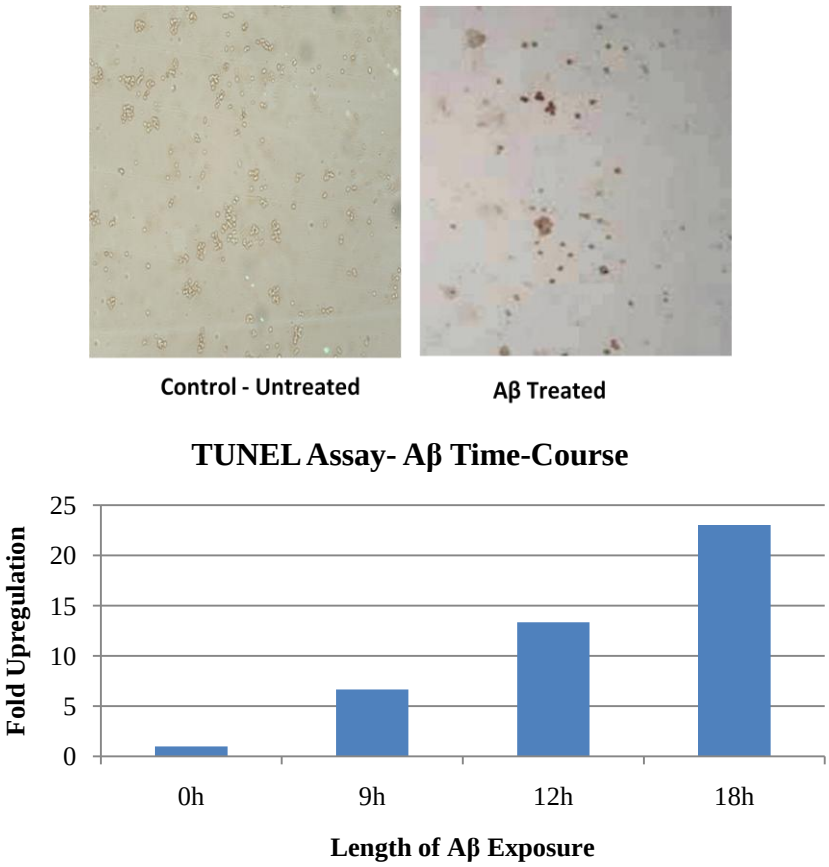

Figure-10: Aβ Time-Course for TUNEL Assay *In Vitro*. Upper Panel: Microscope images of untreated control cells (left) and Aβ-treated SHSY cells (right). **Lower Panel:** Quantitiation of the TUNEL assay for one experiment.

To determine whether hEPN-1 treatment can lower SHSY TUNEL staining when added simultaneously or post-insult, we treated five flasks at the time of cell plating with Aβ. One flask was untreated as a negative control. To some Aβ-treated cultures we added hEPN-1 simultaneously, or at 9, 12, or 18 hrs post-insult (**Figure-11**). All flasks were incubated a total of 36 hrs, then the cells were assayed by TUNEL staining. Three independent trials (histoplot) showed a significant (95% confidence) upregulation of apoptosis in Aβ treated cells, and a significant downregulation of apoptosis in all hEPN-1-treated cells. Therefore, hEPN-1 is capable of reversing the Aβ-induced TUNEL staining, even when added 18 hrs post-insult.

Thus, hEPN-1 is able to block cell death (previous data) and an end stage marker of apoptosis (DNA fragmentation) well after apoptotic pathways have initiated.

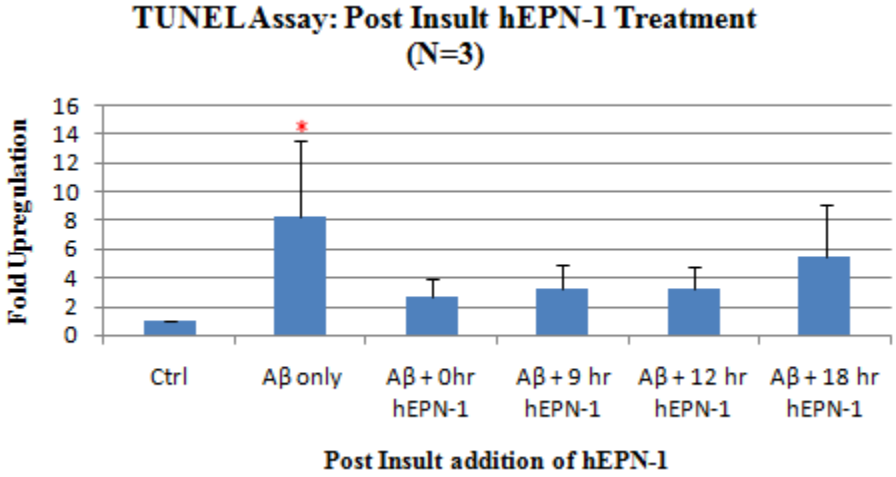

Figure-11: Effects of hEPN-1 Treatment on TUNEL Staining. Quantification of the TUNEL assay with SHSY cells treated for 36 hrs with Aβ, or simultaneously with Aβ and hEPN-1, or with hEPN-1 at various times post-insult. Histobars denote the average of 3 independent trials. Error bars represent one standard deviation. * Indicates Aβ significance from all other groups at the 95% confidence level using a one way ANOVA followed by HSD post-hoc tests.

Caspase-8 Experiments *In Vivo*

Previous experiments in our lab (Kapoor, 2007) indicated that Aβ treatment of SHSY cells increases the cellular levels of caspase-2, an initiator caspase in the *extrinsic* pathway, whose levels are also lowered with hEPN-1 treatment. To extend this finding, we chose to analyze a different initiator caspase in the extrinsic pathway, caspase-8. Although the caspase-8 antibody tested in this thesis gave no detectable signal for human SHSY lysates, it did provide a robust signal for mouse brain lysates. Brain lysates prepared from transgenic AD mice treated with vehicle (dH_2O) or hEPN-1, and analyzed by immunoblots (**Figure-12**) showed a band of the expected 43 kDa size (upper blot). The band disappeared in a negative control lacking primary antibody (lower blot), so it appears to be specific to the primary antibody. The β-tubulin

band intensity (load control) was equal for all samples. The band intensity appeared to be weaker in the hEPN-1 treated mice (three right half lanes) compared to vehicle treated mice (three left half lanes). Quantification of the data (histoplot, 3 mice per group) showed greater than 2 fold downregulation of caspase-8 levels in Alz mice treated with hEPN-1 (right histobar) compared to those treated with vehicle (left histobar). The decrease in caspase-8 signal was significant (95% confidence) using an unpaired 2 tailed T-test. Therefore, this data indicates that oral administration of hEPN-1 at 30 mg/kg for two weeks in 8 month old animals helps cause a downregulation of brain caspase-8 levels *in vivo.*

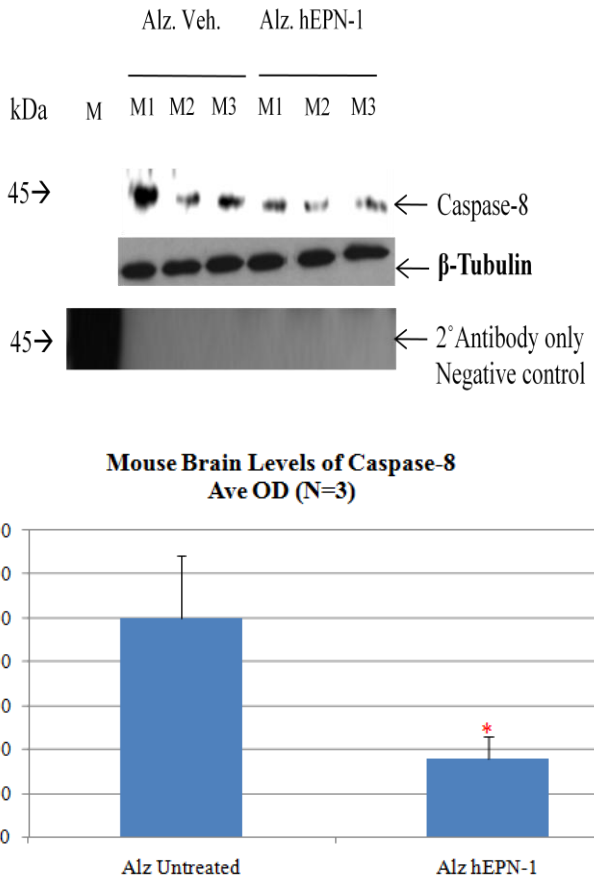

Figure-12: Decrease in Brain Levels of Caspase-8 in Alzheimer's Mice Treated with hEPN-1. Upper Panel: The upper blot is a caspase-8 immunoblot using an antibody that detects caspase-8 at ~43 kDa. "M" denotes a biotinylated size marker. The middle blot is a β-tubulin immunoblot run as a load control. The lower blot is a negative control lacking primary antibody. All blots were run simultaneously with the same 20 µg protein load. **Lower Panel:** Quantification of the caspase-8 levels. Histobars denote the average of 3 mice per group. Errors bars represent one standard deviation. * Indicates significance at the 95% confidence level using an unpaired, two-tailed T-test.

cIAP Experiments

Although our lab's data indicate that hEPN-1 treatment can restore SHSY cell survival against an Aβ challenge, and can lower the cellular levels of caspase enzymes and TUNEL staining, we have no data on the *mechanism* of apoptotic blocking. As discussed in Background, cellular inhibitors of apoptosis (cIAP) are a family of proteins that function to physically bind specific caspases to block their activity and induce their degradation. We chose to assay the cellular levels of cIAP using immunoblots with an antibody that detects cIAP-1 and -2, two isoforms of the same molecular weight. Initially, a hEPN-1 time-course experiment was performed (**Figure-13**) to identify an incubation time where elevations in cIAP levels might be observed. SHSY cells were treated with 150 μM of hEPN-1, a dose previously shown to aid cell survival, and incubated for various time periods. After the incubation period, whole cell lysates were prepared and assayed on immunoblots using an antibody capable of detecting cIAP-1/2 as a single ~69 kDa band. The results showed a 45 kDa band, unexpected in size, whose intensity increased with time of hEPN-1 treatment (upper blot). The band disappeared in a negative control lacking primary antibody (lower blot), indicating that this band interacts with the primary antibody, so likely it is cIAP-related, so here we will refer to it as cIAP-related. In a load control experiment, β-tubulin showed similar band intensities (middle panel). The increase in cIAP-related protein levels was maximal at 72 hrs. Quantification of the signals (histoplot) in three independent trials showed a significant ~2 fold upregulation (95% confidence using HSD posthoc analysis) of cIAP1/2 levels at 72 hrs compared to the untreated control. Thus, treatment of SHSY cells with hEPN-1 at this dose (150 μM) may indeed increase cIAP-1/2-related protein levels *in vitro.* And the upregulation of cIAP-1/2 occurs even in the absence of Aβ, indicating hEPN-1 may be stimulating an Aβ-independent cell survival pathway.

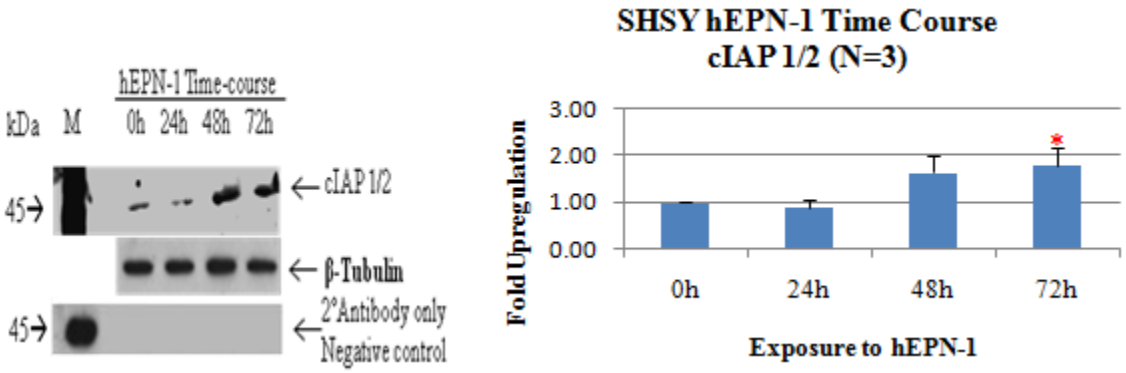

Figure-13: Time-Course of hEPN-1 Increase in cIAP-1/2-Related Protein Levels *In Vitro*. Left Panel: The upper blot is a cIAP-1/2 immunoblot using an antibody that detects both cIAP-1 and -2 as a single band. "M" denotes a biotinylated size marker. The middle blot represents a β-tubulin immunoblot run as a load control. The lower blot is a negative control lacking primary antibody. All blots were run simultaneously with the same 20 µg protein load. **Right Panel:** Quantification of cIAP-1/2 bands. Histobars denote the average of 3 independent trials. Errors bars represent one standard deviation. * Indicates significance from untreated 0 hr control at the 95% confidence level using a one way ANOVA followed by HSD post-hoc tests.

To determine whether the addition of Aβ hinders the upregulation of cIAP-1/2, the experiment was repeated using cells treated with Aβ alone, or with a combination of Aβ and hEPN-1 (**Figure-14**). Quantification of the data from five independent trials showed that Aβ treatment alone did not appear to change the levels of cIAP-1/2-related protein relative to the untreated control, nor did the presence of Aβ alter the ~3.7 fold upregulation of cIAP-1/2 levels induced by hEPN-1. These data indicate that the ability of hEPN-1 to restore cell survival when challenged with Aβ is likely not due to a direct interaction of Aβ and hEPN-1 to interfere with the binding of Aβ to its receptors, but instead indicate that hEPN-1 may upregulate a cell survival pathway.

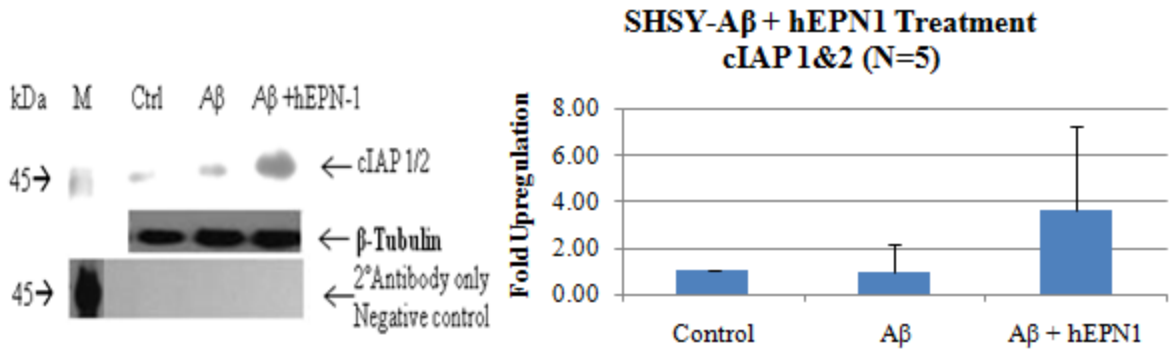

Figure-14: hEPN-1 Upregulates cIAP-1/2-Related Protein Even in the Presence of Aβ. Left Panel: The upper blot is a cIAP-1/2 immunoblot using an antibody that detects both cIAP- and -2 as a single band. "M" denotes a biotinylated size marker. The middle blot is a β-tubulin immunoblot run as a load control. The lower blot is a negative control lacking primary antibody. All blots were run simultaneously with the same 20 µg protein load. **Right Panel:** Quantification of cIAP-1/2 bands. Histobars denote the average of 5 independent trials. Errors bars represent one standard deviation.

To determine whether hEPN-1 treatment can upregulate cIAP levels *in vivo*, immunoblots were performed on whole brain lysates from 8 month old transgenic AD mice treated orally for 2 weeks with vehicle or with hEPN-1 conjugated to a carrier to allow its passage across the blood brain barrier (**Figure-15**). In this case, the blots showed a band of the *expected* 69 kDa size whose intensities were stronger in the hEPN-1-treated mice compared to vehicle-treated mice (upper blot). The β-tubulin load control showed no observable differences in band intensities (middle blot). The 69 kDa band disappeared in a negative control lacking primary antibody (lower blot), so likely the band interacts with the primary antibody. Quantification of the data (histoplot) using three mice per experimental group showed that the hEPN-1 treatment significantly (95% confidence) increased cIAP-1/2 levels ~5.2 fold relative to vehicle-treated mice. Therefore, this data indicates that oral delivery of hEPN-1 (conjugated to a BBB carrier) to 8 month old AD mice can upregulate the cellular brain levels of cIAP-1/2 *in vivo.*

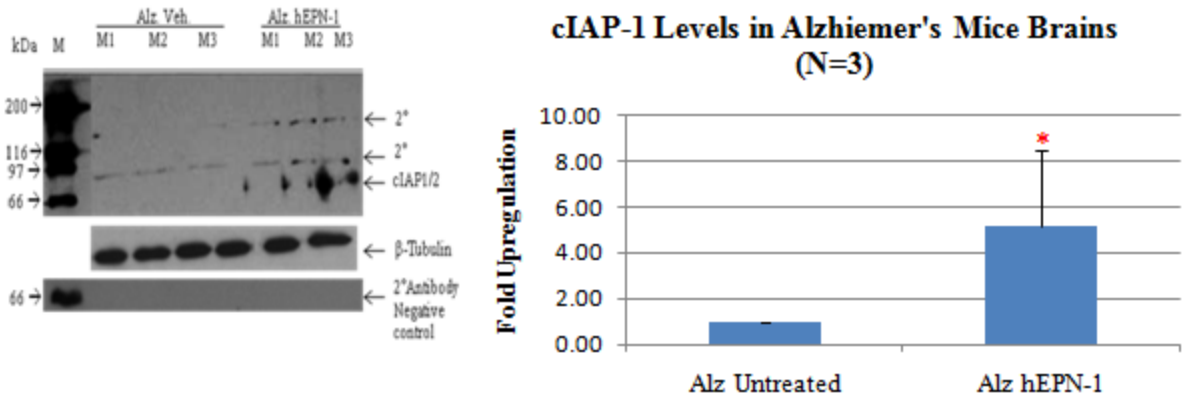

Figure-15: Increase in Brain cIAP-1/2 Levels in Alzheimer's Mice Treated with hEPN-1. Left Panel: The upper blot is a cIAP immunoblot using an antibody that detects cIAP-1 and -2 isoforms as a single ~69 kDa band. "M" denotes a biotinylated size marker. The middle blot is a β-tubulin immunoblot run as a load control. The lower blot is a negative control lacking primary antibody. All blots were run simultaneously with the same 20 µg protein load. **Right Panel:** Quantification of cIAP-1/2 bands. Histobars denote the average of 3 mice per group. Errors bars represent one standard deviation. * Indicates significance at the 95% confidence level using an unpaired, two-tailed T-test.

DISCUSSION

Caspase-9 *In Vitro*

Previous work in our laboratory showed that cellular levels of caspases-2 and -3 are upregulated when human neuronal SHSY cells are treated with Aβ, and this upregulation is reversed with the addition of hEPN-1 (Kapoor, 2007). Caspase-2 is an initiator caspase in the *extrinsic* apoptotic pathway, and caspase-3 is an end stage effector caspase, so the data suggested that Aβ treatment of neuronal cells leads to cell death by activating an *extrinsic* apoptotic pathway. To determine whether the Aβ treatment may also activate an *intrinsic* apoptotic pathway, cellular levels of caspase-9 were analyzed. The immunoblot using a primary antibody produced a band of the expected 46 kDa size. An Aβ time-course experiment showed a clear increase in caspase-9 levels at all times tested (although not statistically significant), while a second Aβ experiment showed no increase. To determine whether the Aβ batch had become inactive, the cellular levels of caspase-3 (previously assayed in our lab) were assayed, and the data indicated strong significant increases in caspase-3 levels in cells treated with Aβ, thus the Aβ batch used in the second caspase-9 experiment discussed above was active. Further experiments would be required to solve this discrepancy. However, the caspase-9 data did show a significant *reduction* in caspase-9 levels in cells treated with both Aβ and hEPN-1, showing that hEPN-1 can strongly affect the *intrinsic* apoptotic pathway.

TUNEL Assay *In Vitro*

A TUNEL assay was used to measure nuclear DNA fragmentation, a hallmark end-stage marker of apoptosis. The data showed that Aβ treatment of SHSY cells for various times showed a clear increase in TUNEL staining as time increased (single experiment). In three independent experiments where all flasks were incubated for 36 hrs, the data showed a significant (95% confidence) upregulation of TUNEL staining in cells treated with Aβ. This data provides a strong validation that true apoptosis occurs in our *in vitro* AD model, and provides evidence of an apoptotic event other than caspase enzyme levels.

Previous data (Ronayne, 2008) showed that simultaneous addition of Aβ and hEPN-1, or hEPN-1 added at 3 and 6 hours post-Aβ to SHSY cells, significantly decreased the TUNEL signal relative to Aβ alone. This thesis explored whether the SHSY cells could be rescued from Aβ when adding the hEPN-1 at greater than 6 hours post-Aβ. Simultaneous or post-treatment of the cells at 9, 12 and 18 hours with Aβ and hEPN-1 was found to significantly (95% confidence using HSD posthoc analysis) decrease the TUNEL signal, showing that hEPN-1 may block apoptosis as part of its mechanism of inhibiting Aβ-induced cell death. Although the inhibition was maximal when hEPN-1 was added simultaneously as the Aβ, because the hEPN-1 could lower the TUNEL staining even when added up to 18 hrs post-Aβ, hEPN-1 may block an end-stage mediator of apoptosis.

Caspase-8 *In Vivo*

To expand the number of caspase species analyzed in our AD models, the cellular levels of caspase-8 were analyzed. Caspase-8 is an initiator caspase in the *extrinsic* pathway. The antibody used in our immunoblot analysis detected no observable bands in SHSY lysates, thus

another primary antibody needs to be tested here. However analysis of whole brain lysates from transgenic AD mice showed a band of the expected 43 kDa size. The intensity of the caspase-8 band significantly decreased (95% confidence using HSD posthoc analysis) in 8 month old mice (an age in which Aβ formation is readily detectable; Jankowsky *et al*., 2001; 2004) orally treated for 2 weeks with hEPN-1 conjugated to a BBB carrier. This *in vivo* caspase-8 data supplements previous *in vivo* data in our lab (Ronayne, 2008) showing that the hEPN-1 treatment significantly lowers brain levels of caspase-7.

cIAP's *In Vitro* and *In Vivo*

Although our previous data showed that hEPN-1 treatment of SHSY cells completely or partially, depending on the dosage, restores cell survival against an Aβ challenge (Stovall, 2006), we had no data on the *mechanism* used to aid cell survival. Cellular inhibitors of apoptosis (cIAP) are a family of proteins that physically bind to specific caspase enzymes to block their activity and cause their degradation (discussed in Background). We analyzed the cellular levels of cIAP using an antibody that detects cIAP-1 and -2 as a single band on gels. The data showed an increase in cIAP levels in SHSY cells (not statistically significant), and in transgenic AD mice (statistically significant, 95% confidence), treated with hEPN-1. The SHSY immunoblots gave a band at ~45 kDa, which is *different* than the expected 69 kDa size, but since the band was only visible in the presence of primary antibody, we assume that it is cIAP-related. The mouse brain lysates produced a band at the *expected* size. The cIAP data shows for the first time that hEPN-1 may aid neuronal cell survival by upregulating proteins known to bind to specific caspases. The cIAP-1/2 upregulation by hEPN-1 occurred in the presence or absence of Aβ, indicating that hEPN-1 likely does not block cell death by *directly* interfering with the interaction of Aβ with its

cell surface receptors, but instead hEPN-1 may activate an independent cell survival signal transduction pathway in neuronal cells.

Future Work

The work done in this thesis has laid the ground work for several future experiments. This is the first time that either an *intrinsic* apoptotic pathway (mitochondrial stress, caspase-9) or a beneficial *caspase inhibitor* pathway (cIAP) have been studied, so there is still much work that could be done on both. With respect to caspase-9 (initiator caspase in the intrinsic mitochondrial stress pathway), *in vivo* studies need to be performed on mouse brains. Analyzing the *intrinsic* ER stress apoptotic pathway using marker caspase-12 would also be interesting as that pathway may also be activated by Aβ.

With respect to caspase inhibitors, some reviews indicate that cIAP levels are strongest in kidney, small intestine, liver and lung (Young *et al.*, 1999; Deveraux and Reed, 1999). This indicates that other tissues besides brain are capable of upregulating cIAPs, so it would be interesting to test other tissues of the transgenic AD mice that secondarily show deterioration with age to compare the hEPN-1 response to neural tissue. In addition, as stated in the Background, some cIAP's (and related families) can act as oncogenes by permanently suppressing cell death (Zender *et al.*, 2006; Hunter *et al.*, 2007). So now that we have found that cIAPs are upregulated by hEPN-1, it will also be important to assay for any uncontrolled cell division (assaying brain tumor formation) or inflammation (monitoring NF-κB activation). If such activities are found, perhaps they could be contained by adjusting the hEPN-1 dose.

In addition, although the observed cIAP band size was the expected 69 kDa in mouse brain, it was an unexpected 45 kDa in SHSY cells. This discrepancy could be further tested by

analyzing a different neuronal cell line (such as rat PC-12 cells), by trying primary mouse brain cultures, by trying a different primary antibody, or by sequencing the immunoprecipitated 45 kDa band to prove it is truly cIAP.

In addition, some Bcl-2 family members are known to be anti-apoptotic (Yuan and Yankner, 2000); they inhibit other pro-apoptotic members of the Bcl-2 family and thereby increase cell survival. Therefore, these BCL-2 family members could be assayed by immunoblots to determine whether they play a role in hEPN-1-induced cell survival.

With respect to the caspase-8 studies, this thesis showed strong *in vivo* data, but no signal was observed with our primary antibody in SHSY lysates. So a different primary caspase-8 antibody should be tested *in vitro*. *In vivo,* other members of the caspase family of enzymes should also be analyzed (if primary antibodies allow), including caspase-2 (previously analyzed *in vitro*), caspase-3 (previously analyzed *in vitro*), caspase-10 (an initiator caspase of the extrinsic pathway), and caspase-12 (an initiator caspase of the intrinsic ER stress apoptotic pathway). The *in vivo* studies should contain more mice than 3 per group (although mouse AD ageing experiments are expensive) to allow for greater variability within an experimental group. Lysates should be stored in small aliquots to prevent degradation.

An extremely intriguing future experiment would be to perform behavioral studies on Alzheimer's mice treated with hEPN-1 to compare with untreated AD mice or WT mice. The experiments could test for learning and memory impairments/recoveries at different ages, as was performed for this AD strain (Reiserer *et al.*, 2007).

A substantial amount of time of this thesis was spent optimizing the TUNEL assay, even though the thesis extended earlier TUNEL experiments performed in our laboratory (Ronayne, 2008). This assay was not successful each time it was performed due to its very long procedure

and large number of steps, but when it was successful it gave excellent data. With respect to more *in vitro* TUNEL studies, different doses of Aβ and hEPN-1 could be tested to optimize the best dose of hEPN-1 for reversing apoptosis. It would also be interesting to check the time point at which hEPN-1 is no longer able to rescue cells. The TUNEL assay has not yet been tested in our *in vivo* AD model. Different areas of the brain could be compared to see where the highest level of apoptosis takes places in the brain, or to see whether the hEPN-1 therapy is area-specific.

To conclude, this thesis demonstrated the involvement of an *intrinsic* mitochondrial stress apoptotic pathway (caspase-9 as marker) in AD models, and its partial blockage by hEPN-1. It expanded the number of caspase species analyzed in the models to include caspase-8. It demonstrated apoptosis beyond levels of caspase enzymes to include DNA fragmentation (TUNEL staining), and its reversal by hEPN-1. And it showed the upregulation of cIAPs by hEPN-1, in the presence or absence of Aβ, indicating hEPN-1 may activate a therapeutic pathway to block cell death.

Alzheimer's disease is the most prevalent neurodegenerative disease worldwide, and is the sixth leading cause of death in the United States. Currently, there is no known cure for AD, and the five current FDA approved drugs temporarily treat mild to moderate symptoms of the disease, but not the underlying neurodegeneration. Thus it is important to develop neuroprotective or neurorestorative therapies. This thesis, combined with previous work in our lab, has shown promising results with respect to hEPN-1 neuroregeneration in *in vitro* and *in vivo* AD models.

BIBLIOGRAPHY

Adams D, Shashoua V (1994) Cloning and sequencing the genes encoding goldfish and carp ependymin. *Gene*, **141**: 237-241.

Adams D, Kiyokawa M, Getman M, Shashoua V (1996) Genes encoding giant danio and golden shiner ependymin. *Neurochemical Research*, **21**: 377-384.

Adams DS, Hasson B, Boyer-Boiteau, A, El-Khishin A, Shashoua VE (2003) A peptide fragment of ependymin neurotrophic factor uses protein kinase C and the mitogen activated protein kinase pathway to activate c-Jun N-terminal kinase and a functional AP-1 containing c-Jun and c-Fos proteins in mouse NB2a cells. *Journal of Neuroscience Research*, **72**: 405-416.

Alzheimer's Association (2009) Alzheimer's Facts and Figures. Accessed 11 June, 2009. http://www.alz.org/alzheimers_disease_facts_figures.asp

Apostolopoulos J, Sparrow RL, McLeod JL, Collier FM, Darcy PK, Slater HR, Ngu C, Gregorio-King CC, Kirkland MA (2001) Identification and characterization of a novel family of mammalian ependymin-related proteins (MERPs) in hematopoietic, nonhematopoietic, and malignant tissues. *DNA Cell Biology*, **20**: 625-635.

Armstrong RA (2006) Plaques and tangles and the pathogenesis of Alzheimer's disease. *Folia Neuropathologica*, **44 (1)**: 1-11.

Bachurin S, Bukatina E, Lermontova N, Tkachenko S, Afanasiev A, Grigoriev V, Grigorieva I, Ivanov Y, Sablin S, Zefirov N (2001) Antihistamine agent Dimebon as a novel neuroprotector and a cognition enhancer. *Annals of the New York Academy of Sciences*, **939**: 425–435.

Barinaga M (1994) Neurotrophic factors enter the clinic. *Science*, **264**: 772-774.

Benowitz LI, Shashoua VE (1997) Localization of a brain protein metabolically linked with behavioral plasticity in the goldfish. *Brain Research*, **11 (2)**: 227-242.

Bratton SB, Walker G, Srinivasula SM, Sun XM, Butterworth M, Alnemri ES, Cohen GM (2001) Recuritment, activation and retention of caspase-9 and -3 by Apaf-1 apoptosome and associated XIAP complexes. *The EMBO Journal*, **20**: 998–1009.

Calbiochem (2000) *Biologics*, Volume **26**, Number 2.

Chartier-Harlin M, Crawford F, Houlden H, Warren A, et al. (1991) Early-onset Alzheimer's disease caused by mutations at codon 717 of the β-amyloid precursor protein gene. *Nature*, **353**: 844-846.

Connor B, Dragunow M (1998) The role of neuronal growth factors in neurodegenerative disorders of the human brain. *Brain Research Reviews*, **27**: 1-39.

Crook NE, Clem RJ, Miller LK (1993) An apoptosis-inhibiting baculovirus gene with a zinc finger-like motif. *Journal of Virology,* **67**: 2168-2174.

Deveraux QL, Reed JC (1999) IAP family protein-suppressors of apoptosis. *Genes and Development,* **13**: 239-252.

Doody RS, *et al* (2008) Effect of dimebon on cognition, activities of daily living, behaviour, and global function in patients with mild-to-moderate Alzheimer's disease: A randomised, double-blind, placebo-controlled study. *Lancet,* **372**: 207–215.

Du C, Fang M, Li Y, Li L, and Wang X (2000) Smac, a mitochondrial protein that promotes cytochrome c-dependent caspase activation by eliminating IAP inhibition. *Cell,* **102**: 33-42.

Duckett CS, Nava VE, Gedrich RW, Clem RJ, Van Dongen JL, Gilfillan MC, Shiels H, Hardwick JM, Thompson CB (1996) A conserved family of cellular genes related to the baculovirus IAP gene and encoding apoptosis inhibitors. *The EMBO Journal*, **15**: 2685-2694.

Fan TJ, Han LH, Cong RS, Liang J (2005) Caspase family proteases and apoptosis. *Acta Biochemica et Biophysica Sinica*, **37 (11)**: 719-727.

Ferrer I, Lopez E, Pozas E, Ballabriga J, Marti E (1998) Multiple neurotrophic signals converge in surviving CA1 neurons of the gerbil hippocampus following transient forebrain ischemia. *Journal of Comparative Neurology,* **394**: 416-430.

Fuentes-Prior P, Salvesen GS (2004) The protein structures that shape caspase activity, specificity, activation and inhibition. *Biochemical Journal*, **384**: 201-232.

Games D, Adams D, Alessandrini R, Barbour R, *et al*. (1995) Alzheimer-type neuropathology in transgenic mice over-expressing V717F β-amyloid precursor protein. *Nature,* **373**: 523-527.

Goate A, Chartier-Harlin M, Mullan M, Brown J, et al. (1991) Segregation of a missense mutation in the amyloid precursor gene with familial Alzheimer's disease. *Nature*, **349**: 704-706.

Goedert M , Spillantini MG (2006) A century of Alzheimer's disease. *Science,* **314**: 777-781.

Green DR, JC Reed (1998) Mitochondria and apoptosis. *Science,* **281**: 1309-1312.

Grigorev VV, Dranyi OA, Bachurin SO (2003) Comparative study of action mechanisms of dimebon and memantine on AMPA- and NMDA-subtype glutamate receptors in rat cerebral neurons. Bulletin of Experimental Biology and Medicine, **136**: 474–477.

Hardy J, Selkoe DJ (2002) The amyloid hypothesis of Alzheimer's disease: progress and problems on the road to therapeutics. *Science*, **297**: 353-356.

Hefti F (1997) Pharmacology of neurotrophic factors. *Annual Review of Pharmacology and Toxicology*, **37**: 239-267.

Hunter AM, LaCasse EC, Korneluk RG (2007) The inhibitors of apoptosis (IAPs) as cancer targets. *Apoptosis*, **12**: 1543–1568.

Imbimbo BP (2008) Alzheimer's disease: γ-secretase inhibitors. *Drug Discoveries Today: Therapeutic Strategies*, **5 (3)**: 169-175.

Jankowsky JL, Slunt HH, Ratovitski T, Jenkins NA, Copeland NG, Borchelt DR (2001) Co-expression of multiple transgenes in mouse CNS: a comparison of strategies. *Biomolecular Engineering*, **17(6)**: 157-165.

Jankowsky JL, Fadale DJ, Anderson J, Xu GM, Gonzales V, Jenkins NA, Copeland NG, Lee MK, Younkin LH, Wagner SL, Younkin SG, Borchelt DR (2004) Mutant presenilins specifically elevate the levels of the 42 residue beta-amyloid peptide *in vivo*: Evidence for augmentation of a 42-specific gamma secretase. *Human Molecular Genetics*, **13**: 159-170.

Kapoor V (2007) Mechanism of reversal of Alzheimer's disease Aβ-induced neuronal degeneration in cultured human SHSY cells using a neurotrophic ependymin mimetic. WPI Master's Thesis, July, 2007.

Lermontova NN, Lukoyanov NV, Serkova TP, Lukoyanova EA, Bachurin SO (2000) Dimebon improves learning in animals with experimental Alzheimer's disease. *Bulletin of Experimental Biology and Medicine* **129** (6): 544–546.

Levy E, Carman M, Fernanandez-Madrid I, Power M, Lieberburg I, et al. (1990) Mutation of the Alzheimer's disease amyloid gene in hereditary cerebral hemorrhage, Dutch type. *Science*, **248**: 1124-1126.

Levy-Lahad E, Wasco W, Poorkaj P, Romano DM, Oshima J, Pettingel WH, Yu CE, Jondro PD, Schmidt SD, Wang K (1995) Candidate gene for the chromosome-1 familial Alzheimer's disease locus. *Science*, **269 (5226)**: 973-977.

Lindsay R, Wiegand S, Altar C, DiStefano P (1994) Neurotrophic factors: from molecule to man. *Trends in Neurosciences*, **17**: 182-190.

Liston P, Fong WG, Korneluk RG (2003) The inhibitors of apoptosis: there is more to life than Bcl2. *Oncogene*, **22**: 8568-8580.

Mullan M, Crawford F, Axelman K, Houlden H, Lilius L, Winblad B, Lannfelt L (1992) A pathogenic mutation for probable Alzheimer's disease in the APP gene at the N-terminus of β-amyloid. *Nature Genetics*, **1**: 345-347.

Murrell J, Farlow M, Ghetti B, Benson M (1991) A mutation in the amyloid precursor protein associated with hereditary Alzheimer's disease. *Science*, **254**: 97-99.

New York Times (2007) Antihistamine Shows Promise in Treating Alzheimer's. June 11. http://www.nytimes.com/2007/06/11/business/11drug.html?ei=5090&en=6dd260f0ecf61466&ex=1339214400&partner=rssuserland&emc=rss&pagewanted=print

Rajendran L, Schneider A, Schlechtingen G, Weidligh S, Ries J, Braxmeier T, Schwille P, Schulz JB, Schroeder C, Simons M, et al. (2008) Efficient inhibition of the Alzheimer's disease β-secretase by membrane targeting. *Science*, **320**: 520-523.

Rapoport M, Dawson H, Binder LI, Vitek M, Ferreira A (2002) Tau is essential to β-amyloid-induced neurotoxicity. *Proceedings of the National Academy of Sciences, USA*, **99**: 6364-6369.

Reiserer RS, Harrison FE, Syverud DC, McDonald MP (2007) Impaired spatial learning in the APP+PSEN 1DeltaE9 bigenic mouse model of Alzheimer's disease. *Genes Brain Behavior*, **6**: 54-65.

Roberson ED, Mucke L (2006) 100 years and counting: prospects for defeating Alzheimer's disease. *Science*, **314**: 781-784.

Roberson E, Scearce-Levie K, Palop J, Yan F, Cheng I, Wu T, Gerstein H, Yu G, Mucke L (2007) Reducing endogenous tau ameliorates amyloid-β-induced defecits in an Alzheimer's disease mouse model. *Science*, **316**: 750-754.

Ronayne RE (2008) Human ependymin-1 neurotrophic factor mimetics reduce tau phosphorylation and cellular apoptosis *in vitro* and *in vivo* in Alzheimer's disease models. WPI Master's Thesis, September, 2008.

Rothe M, Pan MG, Henzel WJ, Ayres TM, Goeddel DV (1995) The TNFR2-TRAF signaling complex contains two novel proteins related to baculoviral inhibitor of apoptosis proteins. *Cell*, **83**: 1243-1252.

Roy N, Deveraux QL, Takahashi R, Salvesen GS, Reed JC (1997) The c-IAP-1 and c-IAP-2 proteins are direct inhibitors of specific caspases. *The EMBO Journal*, **16**: 6914-6925.

Russo C, Schettini G, Saido T, Hulette C, Lippall C, Lannfelt L, Ghetti B, Gambetti P, Tabaton M, Teller J (2000) Presenilin-1 mutations in Alzheimer's disease. *Nature*, **405**: 531-532.

Salvesen GS, Duckett CS (2002) IAP Proteins: Blocking the roads to death's door. *Molecular Cell Biology*, **3**: 401-410.

Schenk D, Barbour R, Dunn W, Gordon G, *et al*. (1999) Immunization with amyloid-β attenuates Alzheimer disease-like pathology in the PDAPP mouse. *Nature*, **400**: 173-177.

Shashoua V, Adams D, Boyer-Boiteau A, Cornell-Bell A, Li F, Fisher M (2003) Neuro-protective effects of a new synthetic peptide (CMX-9236) in i*n vitro* and i*n vivo* models of cerebral ischemia. *Brain Research* **963**: 214-223.

Shashoua VE, Adams DS, Volodina NV, Lia H (2004) New synthetic peptides can enhance gene expression of key antioxidant defense enzymes *in vitro* and *in vivo*. *Brain Research* **1024**: 34-43.

Shen L, Figurov A, Lu B (1997) Recent progress in studies of neurotrophic factors and their clinical applications. *Journal of Molecular Medicine*, **75**: 637-644.

Sherrington R, Rogaev EI, Liang Y, Rogaeva EA, Levesque G, Ikeda M, Chi H, Lin C, Li G, Holman K, et al. (1995) Cloning of a gene bearing missense mutations in early-onset familial Alzheimer's disease. *Nature*, **375**: 754-760.

Shi Y (2002) Mechanisms of caspase activation and inhibition during apoptosis. *Molecular Cell*, **9**: 459-470.

Shiozaki EN, Shi Y (2004) Caspases, IAPs, and Smac/DIABLO: mechanisms from structural biology. *Trends in Biochemical Science*, **29**: 486-494.

Srinivasula SM, Hegde R, Saleh A, Datta P, Shiozaki E, Chai J, Lee RA, Robbins PD, Fernandes-Alnemri T, Shi Y, Alnemri ES (2001) A conserved XIAP-interaction motif in caspase-9 and Smac/DIABLO regulates caspase activity and apoptosis. *Nature*, **410**: 112-116.

Srinivasula SM, Ashwell JD (2008) IAPs: What's in a name? *Molecular Cell*, **30**: 123-135.

Stovall K (2006) Partial restoration of cell survival by a human ependymin mimetic in an *in vitro* Alzheimer's disease model. WPI Master's Thesis, August, 2006.

Takahashi R, Deveraux Q, Tamm I, Welsh K, Assa-Munt N, Salvesen GS, Reed JC (1998) A single BIR domain of XIAP sufficient for inhibiting caspases. *Journal of Biological Chemistry*, **273 (14)**: 7787-7790.

Tamaoka A, Odaka A, Ishibashi Y, Usami M, et al. (1994) APP717 missense mutation affects the ratio of amyloid-β protein species ($A\beta_{1-42}$ and $A\beta_{1-40}$) in familial Alzheimer's disease brain. *Journal of Biological Chemistry*, **269**: 32721-32724.

Thornberry NA, Lazebnik Y (1998) Caspases: enemies within. *Nature*, **281**: 1312-1316.

Tuszynski M, Gage F (1994) Neurotrophic factors and diseases and the nervous system. *Annals of Neurology*, **35**: S9-S12.

Uren AG, Pakusch M, Hawkins CJ, Puls KL, Vaux DL (1996) Cloning and expression of apoptosis inhibitory protein homologs that function to inhibit apoptosis and/or bind tumor necrosis factor receptor-associated factors. *Proceedings of the Natural Academy of Science USA*, **93**: 4974-4978.

Vaux DL, Silke J (2005) IAPs, RINGs and ubiquitylation. *Nature Reviews Molecular Cell Biology*, **6**: 287–297.

Walsh DM, Klyubin I, Fadeeva JV, Cullen WK, Anwyl R, Wolfe MS, Rowan MJ, Selkoe DJ (2002) Naturally secreted oligomers of amyloid-β protein potently inhibit hippocampal long term potentiation *in vivo*. *Nature*, **416**: 535-539.

Yan SD, Chen X, Fu J, Chen M, Zhu H, Roher A, Slattery T, Zhao L, Nagashima M, Morser J, Migheli A, Nawroth P, Stern D, Schmidt AM (1996) RAGE and amyloid-β peptide neurotoxicity in Alzheimer's disease. *Nature*, **382**: 685-691.

Yan SD, Bierhaus A, Nawroth PP, Stern DM (2009) RAGE and Alzheimer's disease: A progression factor for amyloid-β-induced cellular perturbation? *Journal of Alzheimer's Disease*, **16**: 833-843.

Yang Y, Fang S, Jensen JP, Weissman AM, Ashwell, JD (2000) Ubiquitin protein ligase activity of IAPs and their degradation in proteasomes in response to apoptotic stimuli. *Science*, **288**: 874–877.

Yang QH, Du C (2004) Smac/DIABLO selectively reduces the levels of c-IAP1 and c-IAP2, but not that of XIAP and livin in HeLa cells. *Journal of Biological Chemistry*, **279**: 16963–16970.

Yankner BA, Duffy LK, Kirschner DA (1990) Neurotrophic and neurotoxic effects of amyloid-β protein: Reversal by tachykinin neuropeptides. *Science*, **250**: 279-282.

Young SS, Liston P, Xuan JY, McRoberts C, Lefebvre CA, Kerneluk RG (1999) Genomic organization of the physical map of the human inhibitors of apoptosis: HIAP1, HIAP2. *Mammalian Genome*, **10**: 44-48.

Yu D, Silva GA (2008) Stem cell sources and therapeutic approaches for central nervous system and neural retinal disorders. *Neurosurgical Focus*, **24 (3-4)**: 1-23.

Yuan J, Yankner BA (2000) Apoptosis in the nervous system. *Nature*, **407**: 802-809.

Zender L, Spector MS, Xue W, Flemming P, Cordon-Cardo C, Silke J, Fan ST, Luk JM, Wigler M, Hannon GJ, et al. (2006) Identification and validation of oncogenes in liver cancer using an integrative oncogenomic approach. *Cell,* **125**: 1253–1267.

Zuccato C, Cattaneo E (2009) Brain-derived neurotrophic factor in neurodegenerative diseases. *Nature Reviews Neurology,* **5**: 311-322.